Scaling up the generation of Metallofullerenes for QIP



Yi Han
St Anne's College
University of Oxford

Submitted for the degree of Master of Science(by research)

Abstract 4
1. Introduction 6
1.1 Endohedral Fullerenes 6
1.2 Nomenclature 7
1.3 Synthesis of endohedral fullerenes 7
1.3.1 Laser Ablation 7
1.3.2 Arc discharge method 8
1.3.3 Ion implantation 8
1.3.4 Other methods 9
1.4 The role of endohedral fullerenes in QIP 9
2. Overview of the endohedral fullerene generation process with arc discharge method 12
2.1 Soot production 12
2.1.1 Arc discharge 12
2.2 Fullerene extraction 14
2.3 The separation/purification of EMFs 15
2.3.1 Liquid chromatography 15
3. Experimental techniques 17
3.1 Arc discharge 17
3.2 Soxhlet extraction method and apparatus 17
3.3 Liquid chromatography 18
3.4 Mass spectrometry 18
4. Optimization of the Soxhlet extraction of fullerenes 20
4.1 Introduction 20
4.2 Work Package 1: Generation of $Y@C_{82}$ 20
4.2.1 Experimental section 20
4.2.2 HPLC separation 22
4.2.3 Results 22
4.2.4 Discussion 24
4.3 Second work package: Additional Generation of $Y@C_{82}$ 26
4.3.1 Introduction 26
4.3.2 Results 27
4.3.3 Discussion 30
4.4 Third Work Package: Soxhlet time optimisation 31
4.4.1 Introduction 31
4.4.2 Results 31

4.4.3 Discussion....33
4.5 Conclusions....35
5. Optimization of emf yield via arc discharge....36
5.1 I ntroduction....36
5.2 2^2 factorial design....37
5.3 Work Package 1....37
5.3.1 Experimental section....38
5.3.2 Results....39
5.3.3 Discussion....39
5.4 Work Package 2....40
5.4.1 Introduction....40
5.4.2 Experimental section....40
5.4.3 Results....41
5.4.4 Discussion....41
5.5 Conclusion....42
6. A study on the fullerene formation mechanisms in the arc discharge method....44
6.1 Introduction....44
6.2 Data....45
6.3 A review on the classic formation mechanisms....45
6.3.1 Pentagon road....45
6.3.2 Fullerene road....46
6.4 Analysis and Discussion....46
6.4.1 New fullerene formation scenario for arc discharge method....48
6.5 Conclusions....50
7. Possible modifications of the arc discharge system....52
7.1 Introduction....52
7.2 Identified issues....52
7.3 Modification of the synthesis of fullerenes process with the pilot system....54
7.3.1 Hoover soot collection....54
7.3.2 The integration of a vacuum filter....54
7.3.3 Attempts to improve the cooling system....55
7.4 New generation of arc discharge system....55
7.5 Conclusions....57
8. $TiCl_4$ based EMF purification method....59
8.1 Introduction....59
8.2 Experimental section....59
8.3 Results....60

8.4 Discussion 62
8.4.1 Residual higher fullerenes 62
8.4.2 The recovery rate of Y@C_{82} 62
8.4.3 The influence of solvents and types of Lewis acids 65
8.4.4 General discussion 65
8.5 Conclusions 66
9. Two-stage Soxhlet Separation Method 67
9.1 Introduction 67
9.2 Experimental section 67
9.3 Results 68
9.4 Discussion 70
9.4.1 The dynamics of the two-stage Soxhlet method 70
9.4.2 The integration of the two-stage Soxhlet extraction method 71
9.4.3 The origin of the separation/purification with the two-stage Sohxlet method 71
9.5 Conclusion 72
10. Other Complimentary activities 73
10.1 Trials of Synthesizing Novel endohedral fullerenes 73
10.1.1 The diversity of endohedral fullerenes 73
10.1.2 Synthetic Strategy 74
10.1.3 Results & Discussion 76
10.2 Functionalization of Endoherdal fullerenes 79
10.2.1 Introduction 79
10.2.2 Experimental section 80
10.2.3 Results 81
10.2.4 Discussion 81
10.2.5 Conclusions 82
11. Conclusions and Future Work 83
References 86

ABSTRACT

Endohedral fullerenes are remarkable molecules with unique electronic, magnetic, photovoltaic and quantum properties. They have found a number of applications in various fields. Among all the potential applications, one particularly interesting application is to employ them as building blocks for a quantum computer. However, the scientific and commercial exploitation of these materials is held back by their low productivity. In this project, the arc discharge synthesis of endoedral fullerenes which remains the most promising candidate for producing bulk quantities of Endohedral Metallofullerenes (EMFs) was divided into 4 steps, and in this thesis, I discuss the attempts that had been made to optimise each of them. In this project, I focus on $Y@C_{82}$, which is a spin active endohedral fullerene with attractive quantum properties. I obtained sights into the dynamics of the Soxhlet extraction of fullerenes, and developed an optimised Soxhlet scheme which is able to extract 95% of $Y@C_{82}$ from the soot within 60 hours (Chapter 4). Further progress on the optimization of Soxhlet extraction was made when a two-stage Soxhlet extraction/purification was independently developed (chapter 9). This method employs two solvents (toluene and DMF) to extract fullerenes with different dipolar moment. It was not only able to extract fullerenes effectively from the soot, but also to purify EMFs/Trimetallic nitride template(TNT) into high purity (97%).

Efforts were made to search for the best conditions for generating $Y@C_{82}$ with a patented pilot arc discharge system. After analysing the data of the yield of fullerenes in various conditions with a "2^2 factorial design of experiment", I believe the yields of $Y@C_{82}$ can be increased by using high He pressure (Chapter 5).

The scaling up the production of EMFs was also tackled from a more fundamental and theoretical aspect. Although fullerenes have been efficiently synthesized by several methods to date, the formation mechanism of these materials remains a mystery. The study of the fullerene formation mechanism in arc discharge is particularly rare due to intrinsic technical difficulties. In chapter 6, I propose a new "bottom up" formation scenario in the arc discharge synthesis of fullerenes that adopts the so called "closed network growth".

Attempts that were made to improve the efficiency and safety of the current system were introduced in Chapter 7. Concepts to develop a more efficient safe arc discharge system were suggested and discussed in the same chapter. The Lewis acid separation method was reported to be an efficient approach to remove the empty cages from the EMFs[1], however, this method is only suitable for a lab equipped with specialized facilities and cannot be characterized as generic (Chapter 8).

Finally, I have applied a functionalization scheme to C_{60} which may be a promising scheme to functionalize spin-active metallofullerenes to produce a two-qubit quantum information system (Chapter 10).

1. INTRODUCTION

1.1 ENDOHEDRAL FULLERENES

Carbon, one of the most abundant elements on this planet, played a unique role in the process of developing of life. In addition to the two well-known allotropes graphite and diamond, in 1985, a third was discovered by Curl, Kroto, Smalley and co-workers during their study of the formation of long-chain carbon molecules in the interstellar space and circumstellar shells.[2] In their study involving the vaporization of graphite by laser ablation, they found a surprisingly stable species consisting of 60 carbon atoms. They proposed a soccer-ball-like structure where 60 carbon atoms are located at each vertex of this truncated icosahedron structure and named it buckminsterfullerene, which has been truncated to fullerene. The discovery of fullerenes led to Kroto, Curl and Smalley being awarded the Nobel Prize in Chemistry in 1996.

Not long after this remarkable discovery, the same research group believed they successfully synthesized a molecule that had a Lanthanum atom captured inside a carbon cage. This new species was made by laser vaporization of a La impregnated graphite disc. This "La+C_{60}" complex was the first so called "endohedral metallofullerene" (EMF) molecule that discovered.[3] The term "endohedral" which originates from a combination of Greek words ("endon" - within and "hedra" – face of a geometrical figure) was introduced by Cioslowski[1] and independently by Schwarz and Kratschmer in 1991.[4,5]

However, La@C_{60}, as it became later known, was not stable in the air.[6] A few years later, further evidence was found to support the existence of this species by showing that LaC_{60}+ ions were inert to H_2, O_2, NO and NH_3 [7].

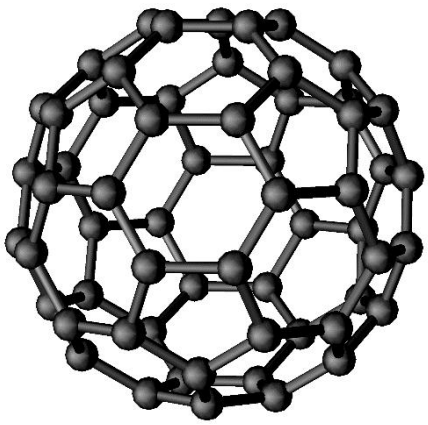


Figure. 1 Schematic of C_{60}[8]

Many atoms and combinations of various atoms were put inside fullerenes cages, and new endohedral fullerene species are still being reported today. The encapsulation of atoms or clusters leads to changes of the cage's chemical and other properties[9,10,11] which makes endohedral fullerenes a class of molecules attractive to scientists for their unique structure. In addition, more and more potential applications of these molecules have been discovered (including MRI contrast agents, energy harvesting in organic solar cells and quantum nanoelectronics) and this trend will probably continue. [11],[12]

However, the lack of availability of these materials remains as one of the main obstacles that impedes further exploitation of these molecules, this issue involving the low productivity of EMF containing soot and extremely time consuming and labour intensive separation/purification method for EMF generation.

This project was designed to address this issue. Specific attention is paid to scaling up the production of spin active endohedral fullerenes via a modified arc-discharge method.

1.2 Nomenclature

Already a few years after the first discovery of C_{60}, more forms of fullerene-based materials had been found. The traditional way of representing an endohedral fullerenes is done by writing the "MC_m" formula, this method became inadequate when representing more complicated fullerene materials, since this nomenclature has no indication of whether the heteroatoms are captured inside the cage or attached to the cage as a functional group. Today, the most commonly used nomenclature for EMF is using the symbol "@" to give an indication that the heteroatoms are encapsulated by fullerenes.[6] A general formula for the new nomenclature can be written as *(captured clusters)*@C_x, e.g., a C_{82} cage with one Yttrium atom inside its sphere can be written as Y@C_{82}. However, the nomenclature suggested by IUPAC is different from the method introduced above. For instance, La@C_{82} is written as "iLaC_{82}" and reads as "[82] fullerene-incar-lanthanum". [13] Nevertheless, the ad-hoc naming method using the @ symbol is now almost universally adopted by fullerene researchers and this thesis stays with this tradition.

1.3 Synthesis of endohedral fullerenes

1.3.1 Laser Ablation

The first EMFs were produced by laser ablation. This method remains as an important route of synthesizing EMFs. In a typical laser ablation process for the production of fullerenes, a target composite of metal oxide and graphite mixture is placed in a furnace at 1200 °C. [14] This target is hit upon by a high frequency Nd:YAG laser at 532 nm in an Ar gas flow. The graphite target is vaporized and soot containing small amounts of EMFs is produced, which flows through the quartz tube with the Ar gas carrier and is condensed on the tube wall. [6,15,16] This technique for fullerene generation is still employed to produce small quantities of EMFs for certain studies. However, the cost of a laser apparatus is high and the yield of EMFs via this method is low, therefore is not suitable for producing EMF in macroscopic quantities. Since the synthesis of C_{60} and the first EMFs via laser ablation, several other fullerene generation methods have been discovered.

1.3.2 Arc discharge method

In the year 1991, Kratschmer, Huffman and Fostiropoulos created a true breakthrough. They developed DC arc-discharge method for fullerene synthesis and later made macroscopic amounts of EMFs. [17,18] Due to the success of this method it is also called as the Kratschmer-Huffman method. In this method, high current is sent to the metal-oxide/graphite composite rods to be used as anodes against a cathode graphite electrode in the presence of He gas. As a result, a high temperature plasma (>2000 ^{o}C) is formed between the composite anode and the cathode.[19,20] At this temperature, graphite is vaporized and various carbon-based structures are formed (including metal carbides), while He acts as a carrier gas. The resulting soot containing empty caged fullerenes as well as EMFs is collected for further processing. The arc-discharge method is a simple and cost-effective method for generating EMFs and has been the workhorse for this science ever since.

Alternative methods, such as the combustion method, have been used extensively to produce empty fullerenes and are capable of producing tons of C_{60} annually, but the arc-discharge method remains by far the most important one for synthesizing EMFs.[21] More recently, modified Kratschmer-Huffman methods have been developed, including the introduction of a nitrogen source to produce Trimetallic Nitride Template (TNT) type fullerenes[10, 22] and the chemically adjusting plasma temperature method to tune the composition of the soot. [23] The generation of EMFs via the arc-discharge method and ways to optimize it are the core of this thesis. As such this method will be discussed in more detail in Chapter 2, below.

1.3.3 Ion implantation

In 1996, another method known as the ion-implantation method was firstly invented by Tellgmann and co-workers.[24] They demonstrated that alkali metal doped EMFs can be synthesized by bombarding the deposited C_{60}-flim with ionized alkali metals under vacuum. However, it was not until 2010, pure alkali metal EMFs were made by ion implantation and isolated, the reason being that EMFs tend to polymerize with the C_{60} matrix.[25]

The basic principle of this technology was to introduce ions into a fullerene rich space in a controlled reaction environment (e.g. by controlling vacuum and temperature), in which ions were allowed to enter the carbon cages. Soon after this production method was established, a similar approach was employed to produce $N@C_{60}$ molecules for the first time. [26] In practice, it is more common that C_{60} cages are destroyed by the incoming nitrogen ions rather than encapsulating them. It is not a surprise that the yield of this method is very low. For instance, in our lab, the typical ratio of $N@C_{60}/C_{60}$ in the product is 10^{-4} to 10^{-5}(on par with the state-of-the-art). Tremendous effort is needed in order to separate and purify the desired species. Therefore, this method is not the best candidate for mass production; however, it remains an efficient way of producing certain fullerene species.

1.3.4 Other methods

Certain endohedral fullerenes including some novel structures have been synthesized in a small scale via a *molecular surgery* route. The first endohedral fullerene synthesized this way was $H_2@C_{60}$. The chemical protocol included opening an orifice in the fullerene cage, followed by pressure treatment and closing of the cage. More recently, $He@C_{60,70}$,[27], $(H_2)_{1,2}@C_{70}$ [28], and $H_2O@C_{60}$[29] have also been successfully produced chemically. This is undoubtedly a very elegant chemical scheme but it is rather hard to produce large amounts of metallofullerenes in this way.

1.4 The role of endohedral fullerenes in QIP

The concept of quantum information process is attractive as an alternative computation approach. Research groups across the world have come up with various approaches to develop quantum computers, such as trapped ions, quantum dots, cavity quantum electrodynamics, liquid-state NMR systems etc. [30]

DiVincenzo[31] stated a set of 5 stipulations for physical implementation of QIP. The value of his work was recognised and the requirements that he suggested were given

the name the DiVincenzo criteria. The 5 criteria are well-known and are quoted verbatim:

1. *A scalable physical system with well characterized qubits;*
2. *The ability to initialize the state of the qubits to a simple fiducial state, such as |000...>;*
3. *Long relevant decoherence times, much longer than the gate operation time;*
4. *A "universal" set of quantum gates;*
5. *A qubit-specific measurement capability.*

The electron/nuclear spin is a quantum property, so that information can be embodied in them, in other words, electron or nuclear spins can be used as quantum bits or qubits.

The idea of liquids-state NMR approach was introduced by Neil Gershenfeld and Isaac Chuang.[30] In this system, the quantum information is embodied in the nuclear spins of the atoms of a molecule. However, NMR-based quantum computers have limited scalability. The limitation in scalability makes this concept is not promising for next generation of computers. Upon the search for candidates that are suitable for QIP, people started to recognise the potential of developing quantum computers based on endohedral fullerenes. As was mentioned previously, endohedral metallofullerenes have electrons donated from the incarcerated atoms to the cage. This electron charge transfer alters the electric and magnetic properties of these molecules and creates stable unpaired-electron systems. The spin relaxation time (T_1) and decoherence time (T_2) of some endohedral fullerenes have been studied and promising results have been published. A pulsed Electron Spin Resonance (ESR) study of T_1 and T_2 over a range of temperatures in toluene, deuterated toluene and deuterated o-terphenyl have been performed by Brown, R. M and co-workers. [9] Generally, T_1 is longer than T_2. In other words, normally, any spin operation is limited by T_2. The idea of using $N@C_{60}$ and $P@C_{60}$ as qubits was suggested by Wolfgang Hartneit. [32] In his model, qubits are addressed and read out by ESR methods. Let us take $N@C_{60}$ as an example. The coherence time (T_2) in $N@C_{60}$ has been measured to be up to 250 microseconds in frozen CS_2 solution at 160K. A typical X-band ESR spectrometer has a nutation period about 30 ns. This corresponds to more than 8,000 Rabi oscillations (spin flips) before decoherence happens. In addition, it has been shown that even with a systematic error in single qubit operation as high as 10%, a fidelity between 0.999 and 0.9999 can still be achieved, and this performance of qubit logic gates when judging quantum computing implementations meets the requirements for quantum error correction. Along with the long T_1 and T_2,

investigation into these molecules has fulfilled the common requirements for fault-tolerant quantum computation. [33,34]

In addition to N@C_{60}'s attractive electron spin properties, its nuclear spin has its own use. The nuclear spin allows even longer storage time of quantum information. The nuclear spin can be operated by radio frequency pulses contrast to microwave pulses for the electron spin. [35] When the nuclear spin is employed, the electron spin cannot only generate ultrafast phase gates, but also protect the nuclear spin qubit from environmental interactions by bang-bang decoupling. [34] By considering the nature of electron spin and nuclear spin of N@C_{60}, and the symbiosis of them, we believe that N@C_{60} and its derivatives are one of the most promising building block for molecular quantum computers.

However, the production and purification of N@C_{60} is extremely tedious and challenging, and it is almost impracticable to produce large enough amounts of pure N@C_{60} even for lab use, let alone commercial utilization. EMFs have the advantage of much faster generation of high purity sample. Some EMFs have showed potential to be selected to develop fault-tolerant quantum computers. [9] It has been reported that under optimized conditions, T_2 for Y@C_{82} can exceed 200 microseconds, and their electron spin can be manipulated within tens of nanoseconds. These properties have made them promising candidates for molecular QIP. [9] However, when EMFs are considered for use as building blocks of quantum computers, EMFs have their own challenges. For instance, the chemistry of EMFs is less well understood compared to that of N@C_{60} which is remarkably similar to well-established C_{60} chemistry. Both for scientific research and for building a scalable quantum computer, there is a strong call for higher availability of EMFs. This is seen as one of the most foremost challenges of developing EMFs–based quantum computing techniques, and this project is designed to address this issue. By considering the properties of various EMFs and the availability of raw materials, Yttrium-based mono-metallofullerenes are selected as the material of choice and the production process of this material is the main object of study in this project.

2. Overview of the endohedral fullerene generation process with arc discharge method

2.1 Soot production

The endohedral fullerene generation process starts with the production of soot. Since the C_{60} was synthesized for the first time by Kroto et al[2], various soot generation methods have been discovered, however, the arc discharge method remains the most important route for synthesizing EMFs, including $Y@C_{82}$ [11].

2.1.1 Arc discharge

A typical arc discharge system consists of a reaction chamber, a pumping system, inert gas supplier and a power supply unit. During the operation, the graphite rod is brought close to the other electrode, a plasma is created by sending high current though the composite rod anode and the cathode, and carbon is vaporised from the composite electrode under high temperature conditions[36].

The concept of a typical arc discharge system is schematically represented in Figure 2.

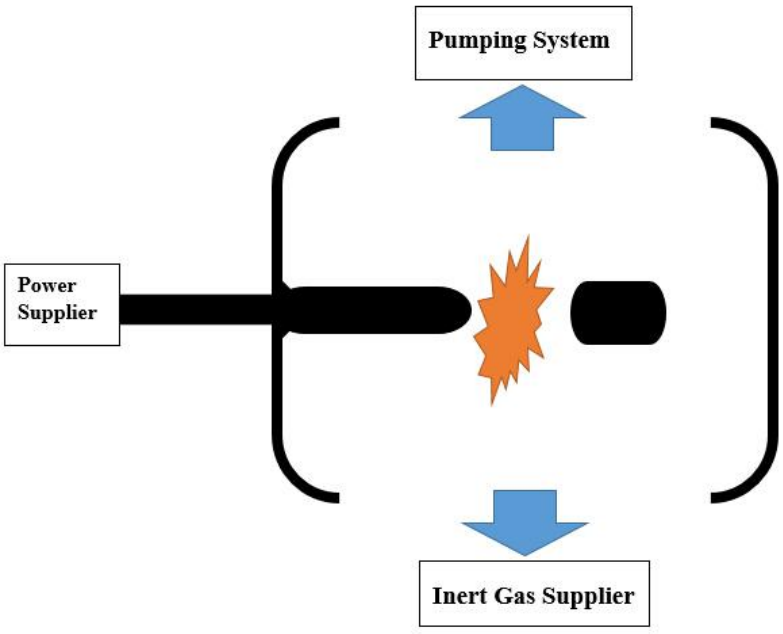


Figure.2 A typical arc discharge system consists of a vacuum chamber which houses two graphite electrodes (the composite anode and the cathode). The chamber is connected to a pumping system, which is able to degas the system to 10^{-4}-10^{-5} torr, and a gas supplier that provides inert gas such as He during the operation.

Endohedral fullerenes can be produced with the same method, simply using heteroatom-doped graphite rods instead of pure graphite rods. As mentioned in previous chapters, EMFs containing nitride clusters, oxide, sulfide clusters can be synthesized by introducing small amount of gaseous components into the reaction chamber or doping the graphite rods with desired compounds.[37,38,39]

2.1.1.1 PILOT ARC DISCHARGE SYSTEM

In practice, the fullerene production process normally takes a day or more, however, the actual burning process only takes 2 hours at most for a typical 2-rod system. This is due to the whole arc discharge process involving tedious non-production procedures, such as assembling/disassembling the arc system (also labour intensive), and degassing. A concept which modifies the current machines, and helps to simplify the production procedure and to improve the efficiency of fullerene generation was suggested by K. Porfyrakis et al. [40] One of the patented concepts is to develop a system that is capable of burning multi-rods in one production session. The realization of this concept allows the modified system to burn more rods in a single session hence minimizing non-production work.

This patent has been partially realised in a pilot arc discharge apparatus in our lab (Figure 3).

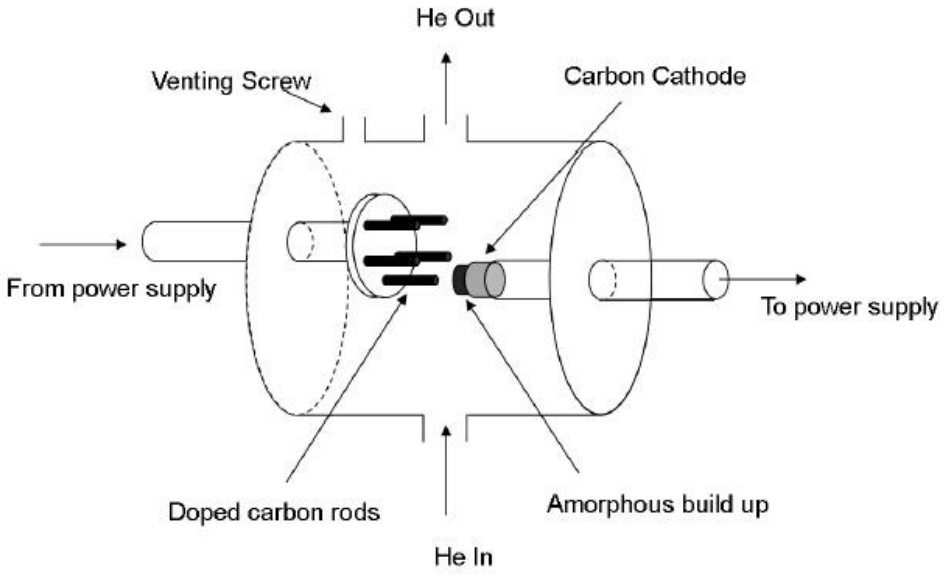


Figure. 3 A schematic diagram of the pilot system.[41]

In the pilot system, a rotation drive is connected to a gas tight feed-though via the door of a stainless-steel chamber. A copper plate which is able to hold up to 6 graphite rods is attached to the rotation drive. A Migatronic TIG LDE 400 welding power supply is attached to the rotation drive which is able to conduct current to the copper plate attached to it and then to the graphite rods. Opposite the rods, a copper electrode is fitted. The chamber is fitted with two outlets which are connected to a He gas supply and a pumping system respectively. The pumping system consists of a diffusion pump and a rotary pump. [36,42,43]

According to the most widely accepted fullerene formation mechanisms, inert gas molecules also work as "carriers" that help vaporized carbon fragments to collide with each other to form fullerenes. Although relatively high He pressure has been used in some cases, [2,44] an inert atmosphere between 40-100 torr has been most commonly reported to be the optimal atmosphere for the highest fullerene yield. [35,43,45] The direct current sent to generate the arc usually in a range 50-500 A.[35,43] However, what combination of values of parameters is the best for our novel pilot arc discharge system is essentially unknown. The first part of this project is designed to determine the best fullerene-yield conditions for the pilot arc-system. This work begun in my co-worker David Barret's Part II thesis.[41] However, that work proved to be incomplete when a better understanding of the Soxhlet extraction method was obtained. For this reason, in this thesis, a study on the Soxhlet extraction process is introduced before studying further the dynamics of the Soxhlet extraction process (Chapter 4). This is despite the fact that fullerene synthesis precedes any fullerene extraction process.

2.2 FULLERENE EXTRACTION

In the process of generating EMFs with the arc discharge method, the production of soot is only the first step. There are various carbon structures present in the soot, including fullerenes, half-formed fullerene fragments, unburned graphite parts and other carbon structures. Fullerene related materials only represent 1-5 % of the soot while in turn EMFs account for less than 20% of the total fullerene product.

The next step in the endohedral fullerene generation process involves isolating fullerenes from the soot. In this section, the two most important fullerene isolation methods are introduced. A unique π-conjugated closed cage structure makes fullerenes soluble in an array of organic solvents such as Toluene and CS_2. The most common solvent extraction routine used today is Soxhlet extraction: soot is contained by a

thimble and solvent is continuously boiled under inert atmosphere, so that hot solvent that is evaporated into the extraction chamber condenses, drops through the thimble and soluble materials (e.g. fullerenes) in the soot are dissolved into the liquid phase.[46] Obtaining solvent free fullerenes can be done by a sublimation method. In this method, the raw soot is heated to high temperature under an inert gas atmosphere. Fullerenes with various sizes and weights start to sublime at different temperatures, mixed fullerenes can be separated into size groups by carefully controlling the temperature, a cold trap is used to collect the sublimating fullerenes.[47] The disadvantage of this method is that the purity of the individual species is relatively low and that it is not suitable for large scale fullerene extraction/purification.[48] The material of focus in this project is $Y@C_{82}$, which is soluble in various organic solvents and can be stored/handled as a solution. Since the solvent extraction method is more suitable for processing bulk materials, Sohxlet extraction is considered more suitable for being employed to extract fullerenes from the soot. A disadvantage of Soxhlet extraction is that it is very time consuming. In addition, the duration of the extraction process is usually decided empirically, and therefore, it is common that soot containing soluble fullerenes is thrown away as a result of insufficient extraction or the fullerene extraction process is unnecessarily long as the soot is over-extracted. To the best of my knowledge, there is no study reported on the dynamics of Soxhlet extraction. Thus, I have carried out a study on the dynamics of the Soxhlet process with the aim to optimize the fullerene extraction stage.

2.3 The separation/purification of EMFs

2.3.1 Liquid chromatography

Chromatography is one of the most common methods for separating mixtures of chemical compounds. This process involves passing the mixture, which is dissolved in a mobile phase, though a stationary phase. The separation of different compounds is based on their different affinity to the stationary phase. Parameters such as polarity, size, shape, electric charge and so on for the different compounds contribute to their different elution time through the stationary phase. [41,49]

In the case of fullerenes, high performance liquid chromatography (HPLC) is the most powerful tool to isolate EMFs and EMF isomers. However, the HPLC purification of EMFs is a highly complex and difficult process. Not only the HPLC apparatus and specialized columns are very expensive, but also the purification of EMFs via HPLC is very time consuming and labour intensive due to the small content of EMFs in the fullerene mixture and the low solubility of EMFs in typical HPLC solvents. Research has been focused in finding new fullerene separation/purification methods to reduce the

dependence on the expensive and slow chromatographic method. One non-HPLC separation method that has been developed involves reacting Lewis acids with the fullerene mixture to precipitate EMFs as an insoluble complex, which can be separated from the solution by filtration. This is a simple, inexpensive, and most scalable candidate.[41,49] I have tested this purification method is tested with my fullerene products.

In addition to my planed work, as the project unfolded, I discovered a modified Soxhlet approach, which is able to significantly enrich the EMFs contents in the raw soot without HPLC; this separation/purification approach is discussed in Chapter 9.

3. EXPERIMENTAL TECHNIQUES

3.1 ARC DISCHARGE

The pilot arc discharge system is the main experimental technique in this project. It was introduced in detail in section 2.1.1.1.

3.2 SOXHLET EXTRACTION METHOD AND APPARATUS

Historically, the fullerenes were extracted with benzene or toluene via a column chromatography method. Later, a hexane solution on neutral alumina method was developed, however, the new method was still considered tedious and solvent-wasteful. Currently, these methods are rarely used. The most common solvent extraction routine used today is Soxhlet extraction: it was introduced briefly in section 2.2.[46] A typical Soxhlet apparatus is shown in Figure 4.

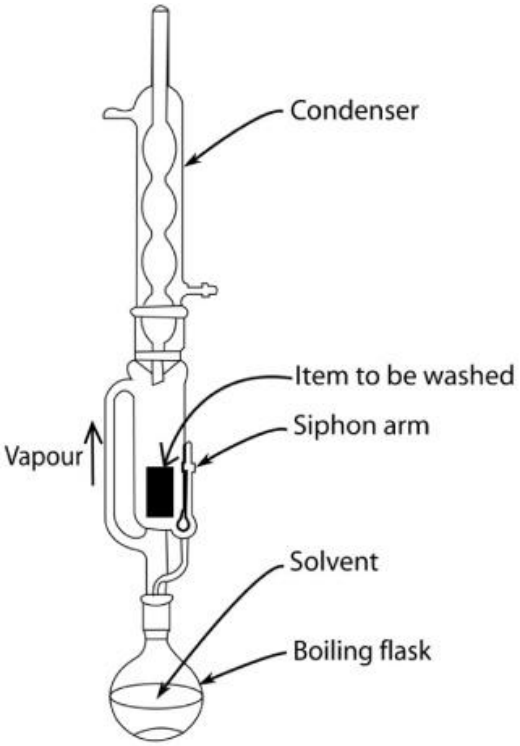


Figure 4. Experimental setup of a typical Soxhlet system.[50]

Toluene, CS_2, N,N-dimethylformamide(DMF) and 1,2-dichlorobenzene (oDCB) are the most commonly used solvents for fullerene extraction. 1,2,4-trichlorobenzene (TCB) is not commonly used regardless of its good affinity towards fullerenes due to its high boiling point and toxic nature. In addition, DMF and pyridine were employed for mono-EMFs as a consideration of high affinity to these materials due to their polar nature.[43] By considering the fullerene affinity to various solvents and their safety implications, DMF is used in our lab for Soxhlet extraction of EMFs. It has been reported that the solvent extraction process may damage endohedral fullerenes, however, C_{82}-type endohedral fullerenes (e.g. Y@C_{82}) are found to be less vulnerable both to air and organic solvents. [48]

3.3 LIQUID CHROMATOGRAPHY

HPLC is the most powerful tool to purify EMFs and separate EMF isomers. In HPLC separation, the fullerene-mixture is combined with a pressurized liquid phase known as eluent and passed through a stationary sorbent phase, which is contained, in a metal column. These chromatography columns are specifically designed to be filled with different types of solid stationary phase (powder or gel) for separating fullerenes. Typically the stationary phase is made of silica gel that is functionalized with aromatic groups. These groups interact strongly with fullerene molecules and allow the retention of fullerenes inside the column. Different fullerene species pass though the column with different speed according to their molecular weight, size, and shape etc. Generally, larger fullerenes travel though the sorbent phase slower than the smaller ones. For EMFs, this is also the case because of their electronic charge on the fullerene cage and strong interaction with the sorbent phase. [41,49] There are different types of columns tailored for separation of certain species or using particular solvent. For instance, Buckyprep-M is more efficient at separating EMFs from the empty cages, while the PPB column (penta-bromobenze) allows various eluents (e.g CS_2, TCB) to be used.[49,11]

3.4 MASS SPECTROMETRY

Mass spectrometry (MS) is a technique that produces spectra of the masses of the molecules comprising a sample of material. This is done by ionizing chemical compounds and separating them in an electric or magnetic field, according to their mass-to-charge ratios. There are several ways to ionize molecules into cations, the most common being: electron impact, chemical ionization, and electrospray.

Ordinary mass spectrum provides information regards to the approximate molecular weight of the molecule, however, the elemental composition of a sample cannot always be deduced based on such information. For example, an ordinary mass spectra reveals a sample's molecular weight is 114, we have no way to know its atomic compositions, and the species could be $C_7H_{14}O$, C_8H_{18}, $C_6H_{10}O_2$ or $C_6H_{14}N_2$. In contrast, high-resolution mass spectrometry is able to measure the molecular weight with much greater accuracy, e.g. 5 decimal places, this techniques allow us to determine the elemental compositions of samples.

In the case of fullerene analysis, the Matrix-Assisted Laser Desorption/Ionization (MALDI) technique is used, working in negative ionization mode with a trans-2-[3-(4-tert-butylphenyl)-2-methyl-2-propenylidene] malononitrile (DCTB) matrix[51].

Initial mass spectrometry analysis was performed at the Department of Chemistry at Oxford with a Waters MALDI Micro MX spectrometer. The resolving power and reliability of this machine was rather limited, it was not uncommon to see a significant shift in the mass spectra (up to 7 m/z had been seen). In order to obtain accurate mass spectra, samples were sent to the National Mass Spectrometry Facility (NMSF) at Swansea, where a Voyager DE-STR spectrometer is used and provides analysis with a much better accuracy. However, it usually took 2 weeks (and up to 2 months) to receive the results back from NMSF, and there was a quota of analyses on the service that was not always sufficient for all group members. The mass spectra included in this thesis were marked either with "NMSF" or "Oxford" to give an indication of the accuracy of the analysis, and for samples marked with "Oxford", an estimation of the error of the mass spectrum is given deduced from the average shifts for the C_{60} and C_{70} peaks in each chart.

4. Optimization of the Soxhlet extraction of fullerenes

I conducted a quantitative study of the Soxhlet extraction process; I determined that the extraction of fullerenes is completed in 100 hrs with DMF. Interestingly, $Y@C_{82}$ is extracted from the soot slightly more readily than C_{60}. In addition, an extraction process which consists of three 20 hours sessions appears to speed up the extraction for both C_{60} and $Y@C_{82}$ up. Finally, I was able to reveal the pattern of the dynamics of Soxhlet extraction of fullerenes under our experimental conditions.

4.1 Introduction

One of the most time-consuming steps of the fullerene generation process is the Soxhlet extraction stage which separates soluble fullerenes form the insoluble soot. Traditionally, the length of Soxhlet extraction has been decided empirically. It can range from 1-2 days to more than 1 week. The reason for this empirical approach is the lack of knowledge on the dynamics of this process. This lack of knowledge leads to great loss of precious fullerenes (if too short) or non-productive work (if too long), and inaccurate conclusions (one example was the study of best yield condition with the pilot arc discharge in this project, this work will be discussed in chapter 5).

The initial goal of this part of the work is to find out the optimal extraction time when DMF is used as a solvent. To my best knowledge, there is no published study on the dynamics of Soxhlet extraction of fullerene method.

4.2 Work Package 1: Generation of $Y@C_{82}$

4.2.1 Experimental section

4.2.1.1 Arc discharge generation of soot

Experiments were carried out with the pilot arc discharge system that I descried earlier. In preparation for soot production, the system was loaded with 6 graphite rods (10x0.9x0.9 cm) doped with 0.8 % wt yttrium, a doping level known to give mono EMFs ($Y@C_{82}$). The system was evacuated to 10^{-4} torr by using a vacuum system consisting of a diffusion pump backed by a rotary pump.

The composite graphite rod was connected to the positive terminal of a Migatronic TIG LDE 400 welding power source and the opposite electrode was connected to the negative terminal of the power source. High current (200 amp) was sent to the rod which was then extended to touch the opposing electrode to generate an arc between them. Once the rod started baking the rod was withdrawn immediately to keep a distance of ~1cm between the rod and the negative electrode. Carbon from the graphite rod began vaporizing in these conditions. During operation, huge amount of heat was generated which warmed up the arc discharge chamber rapidly. To prevent overheating the system, the burning was stopped when a thermometer on the outside surface of the chamber reached 190°C. The burning was resumed when the temperature of the chamber cooled down to 30°C and the polarity of the electrodes of the system were swapped to burn the soot that deposited on the negative electrode. This procedure was repeated until 70-80 % of the rod of the rod was burnt (to prevent intense heat damaging the copper plate that holds the rod). Once the rod was consumed, the copper plate was turned clockwise by rotating the extending shaft until another rod was aligned with the opposite electrode. Vaporization of the second rod resumed and the same procedure was followed for all remaining rods.

After the all the rods inside the arc discharge chamber had been burned, the system was given 2 hours to cool down. Then the side door of the arc discharge chamber was opened and the cover of the lower gas inlet was removed. From that low opening, the soot deposited inside the chamber was "brushed off" and collected in a closed container..

4.2.1.2 SOXHLET EXTRACTION

The collected soot was packed into an extraction thimble with frequent pressing and shaking. The prepared sample was named thimble A. The packed thimble was placed into a Soxhlet apparatus as shown in Figure.3, aluminum foil was used to cover the Soxhlet to isolate it from the ambient environment. The system was connected to N_2 gas flow, The heating mantle was set to level 4.5 (160-170°C) to boil 1 liter of DMF in the lower flask, which was evaporated and condensed on the extraction section and dropped back to the flask through the thimble. A magnetic stirrer was span at 500 rpm to stir the solution.

Heating was stopped after 6 hours whist N_2 continued to flow and the solution was given sufficient time to cool. Once the solution cooled down to room temperature, it was removed and the emptied flask was filled with clear DMF, and the extraction process resumed. This procedure was repeated every 6 hours. After 30 hours of extraction (five 6-hour extraction sessions), the resulting solution had a dark color, which implied that fullerenes kept coming out, in order to speed the experiment up, the solvent was replaced every 12 hours instead of 6 hours. After 102 hours extraction (another six 12 hours extraction session), we found that the resulting solvent still gave a reasonably

dark color, in order to complete the experiment in a reasonable timeframe, we decided to speed the process further by extending each session to 24 hours, and the experiment was stopped after the soot was washed for 198 hours (five 6 hour extraction session + six 12 hours extraction session + four 24 hours extraction session) when the resulting solution from the last session was almost colorless which implied that fullerenes were no longer realised by the soot.

The fullerene-containing DMF solution from each extraction session was dried by a Buchi R-200 rotovap, toluene was added to dissolve the precipitate, and this procedure was repeated 3 times to ensure a complete removal of DMF. Any insoluble material present in the processed solution was removed by passing the solution through a 0.22 micrometer fluoropore filter paper.

4.2.2 HPLC SEPARATION

The filtered solution was concentrated and tested by a JAI LC-9103 HPLC with a Buckyprep-M column (20X250mm). The HPLC measured the amount of light passing through the liquid from a UV light source and generated a real time chromatogram of absorbance against time. The UV light was set to 312 nm which was known to interact with fullerenes. Different compounds were collected according to their retention time of passing though the column.

In this project, the area of C_{60}, C_{70}, higher fulerenes and $Y@C_{82}$ peaks in the HPLC were recorded and converted into mass by employing a formula that developed by our group based on Beer-Lambert's law. The formula was developed by testing an array of samples with known concentrations of a solute with HPLC at a set wavelength, the area of peaks in the HPLC chart is proportional to the amount of UV light adsorbed by the solution at the set wavelength, according to the Beer-Lambert's law, the relationship between the masses of the the solute of the sample and the areas of the corresponding peak in the HPLC chart can be obtained. The procedures were repeated with solutions contain various fullerene species. Formulas for each species of fullernes were developed by calculating the slope of the fitting lines of the absorbance against mass charts for all samples. In this thesis, these calibration formulas are called "F.1".

The accuracy of this measurement is mainly limited by human errors, such as the integration of the peaks in the HPLC chart and the accuracy of the HPLC.

4.2.3 RESULTS

Table 1 below shows how the production yield for C_{60}, C_{70} and $Y@C_{82}$ develops over time with extraction. The results are for the first thimble called Thimble A.

Table. 1 The production yield for fullerenes C_{60}, C_{70} and $Y@C_{82}$ from Thimble A.

Soxhlet time (hrs)	C_{60} (mg)	Progress (C_{60})	C_{70} (mg)	Progress (C_{70})	$Y@C_{82}$ (mg)	Progress ($Y@C_{82}$)
6	0.199	1%	0.030	1%	0.169	7%
12	0.910	7%	0.183	7%	0.125	13%
18	1.250	14%	0.259	16%	0.211	22%
24	1.230	21%	0.198	23%	0.174	30%
30	1.455	30%	0.280	32%	0.121	35%
42	1.226	38%	0.216	39%	0.351	50%
54	1.114	44%	0.197	46%	0.239	60%
66	1.102	51%	0.189	52%	0.134	66%
78	2.471	66%	0.424	67%	0.234	76%
90	0.960	71%	0.171	73%	0.151	83%
102	2.258	85%	0.387	86%	0.282	95%
126	1.562	94%	0.251	94%	0.063	98%
150	0.950	99%	0.150	99%	0.035	99%
174	0.009	100%	0.022	100%	0.011	100%

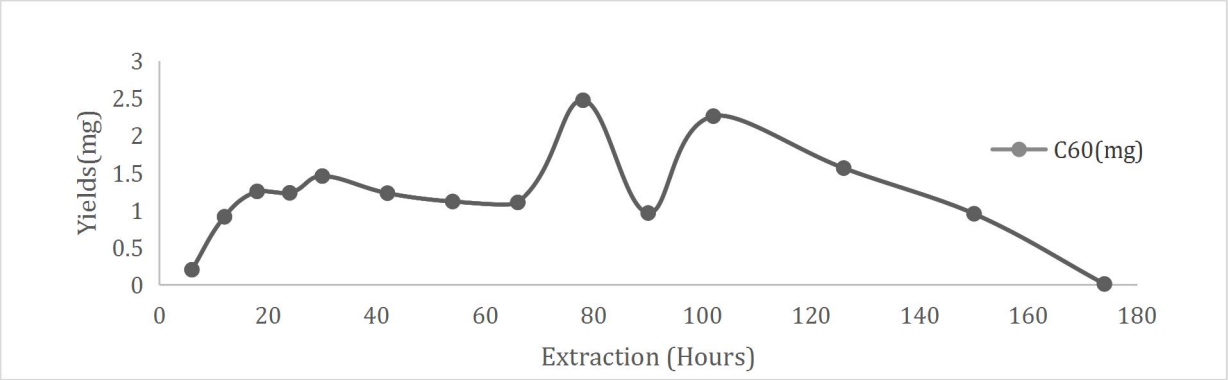
- *The Soxhlet time (hrs) is the time that the soot has been extracted for.*
  C_{60} (mg) represents the amount of C_{60} that was extracted during each extraction session.
  Progress (C_{60}) is calculated by dividing the amount of C_{60} that has been extracted from the soot at the end of each extraction session with the total amount of C_{60} that was extracted from the soot.
- *C_{70} (mg) represents the amount of C_{70} that was extracted during each extraction session.*
  Progress (C_{70}) is calculated by dividing the amount of C_{70} that has been extracted from the soot at the end of each extraction session with the total amount of C_{70} that was extracted from the soot.
- *$Y@C_{82}$ (mg) represents the amount of C_{60} that was extracted during each extraction session.*

Progress ($Y@C_{82}$) is calculated by dividing the amount of $Y@C_{82}$ that has been extracted from the soot at the end of each extraction session with the total amount of $Y@C_{82}$ that was extracted from the soot.

Note: The remaining tables in this chapter have the same structure and notation.

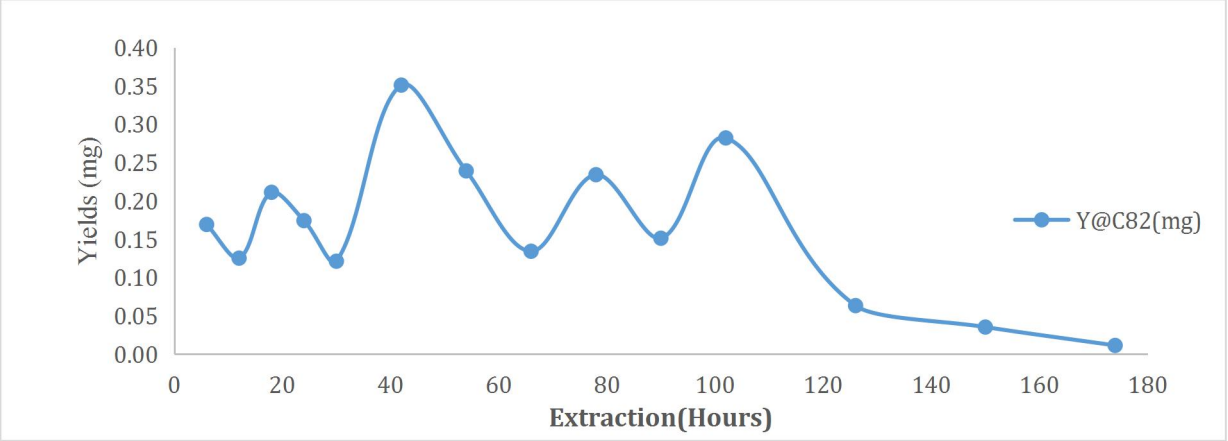
4.2.4 DISCUSSION

The yields for C_{60}, C_{70} and $Y@C_{82}$ from each extraction session are plotted in Figure 5.



(a)

(b)



(c)

Figure. 5 a) The yield of C_{60} from each extraction session as a function of extraction time. b) The yields of C_{70} from each extraction session as a function of extraction time. c) The yields of $Y@C_{82}$ from each extraction session as a function of extraction time.

According to Figure 5, the yields of all the species varied significantly from session to session (when compared to sessions in which the soot was extracted for the same time).

The temperature of the Sohxlet was mainly governed by the temperature of the heater and the frequency of reflux(which was heavily influenced by the N_2 pressure, explained below).

Other factors such as the rotating speed of the magnetic stirrer and ambient temperature could also have influence to the temperature of the Soxhlet. However, the Sohxlet was covered with aluminum foil to isolate it from the ambient environment, the temperature of the heater and the rotating speed of the magnetic stirrer were set constant throughout the experiment, the influence of these factors should be relatively small and unlikely be the reasons for the large variance of the yields from run to run.

One parameter played a role that was more important than I expected is the N_2 pressure, which could significant influence the frequency of the reflux, which in turn effected the temperature of the Soxhlet. The combined effects could lead to considerable variance in the yields. The flow rate of N_2 gas was controlled by a gas valve, which could only adjust the pressure partially. There was an oil reservoir connected to the Soxhlet gas outlet in order to monitor gas flow. However it is not uncommon to see that pressure would be built up in the Soxhlet apparatus. In addition, when another user used the N_2 gas line, the flow rate could be disturbed considerably. The unstable pressure of N_2 in the Soxhlet could affect the boiling point of the solvent, which in turn affects the frequency of reflux (reducing the frequency of reflux from 6 cycles/hour to 1-2 cycles/hour) and the temperature of the working solvent that was wetting the soot. It is worth noting that when the frequency of the reflux was loo low, the main section of the Soxhlet was too cold for any extraction to take place. The concentration of fullerenes in the extracted solution was way below the saturation level, and for all the sessions considered there was no correlation between the saturation level of the solution and the yield.

Despite these uncertainties, it can be noticed that the dynamics of extraction of C_{60} and C_{70} are remarkably close, whereas $Y@C_{82}$ had a very different yield development. The difference in behaviour of C_{60}/C_{70} and $Y@C_{82}$ can be explained by the dissimilar polarity and electric charge property of empty cages and $Y@C_{82}$, i.e. the encapsulated Y^{2+} ion alters its polarity and its chemical property of the carbon cage, and allows the new molecule to have stronger pi-pi interaction with the solvent (DMF). The similarity of the behaviour of C_{60} and C_{70} in the Soxhlet process were confirmed by later experiments; to simplify the discussion, the dynamics of C_{60} will be used to represent the behaviour of

all empty cages in the remaining discussion. The processes of extraction of C_{60} and $Y@C_{82}$ are plotted in Figure 6.

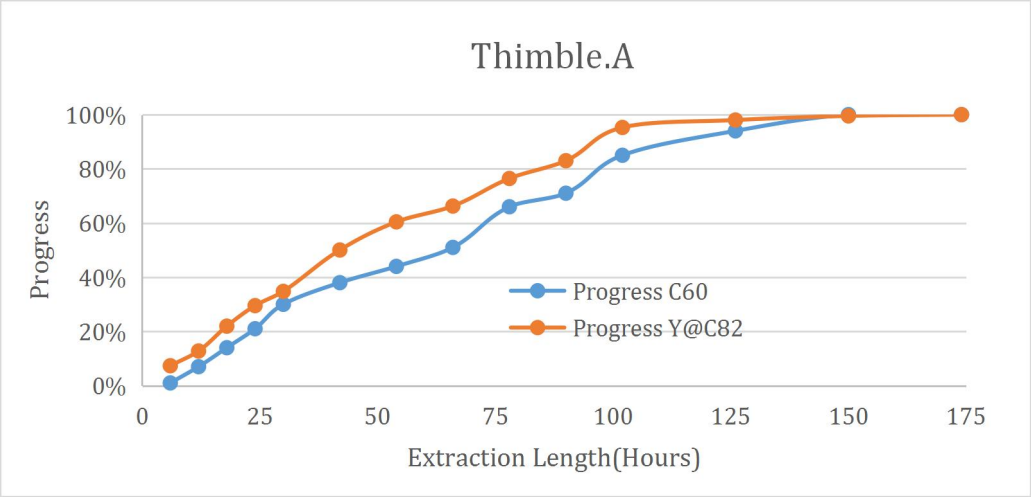


Figure 6. The progress of the extraction of C_{60} and $Y@C_{82}$ of Thimble A against extraction time.

Although the yield of fullerenes from each session is not steady, the process of extraction of $Y@C_{82}$ always precedes that of C_{60}. About 95% of extractable $Y@C_{82}$ was obtained within 102 hours while about 85% of extractable C_{60} was obtained at the same time. The amount of $Y@C_{82}$ that was obtained each time slots after 100 hours extraction decreased considerably while a similar phenomenon of C_{60} is not seen until 156 hours. After 156 hours extraction, there was almost no fullerene mixture in the extracted solvent.

4.3 Second work package: Additional Generation of $Y@C_{82}$

4.3.1 Introduction

In this part of the work, 33 grams of soot were produced via the arc discharge fullerene production as described in 4.2.1.1 with 200 amp current and 50 mbar He.

Since in the extraction of thimble A, it took more than 100 hours to separate 90% of the EMFs from the soot, replacing the solvent every 6 or 12 hour is not necessary. However, it had been noticed that when the soot was extracted for more than 20 hours, the solution became over-saturated due to the diffusion of fine carbon particles into the solvent. As a result, the heater was not able to boil the solution properly, this led to overheating of the solution and reduced the frequency of reflux. By considering both

factors, in the following experiment, each extraction session was timed to be 20 hours max.

In addition, each run of arc discharge is able to produce about 30 g of soot. However, each Soxhlet thimble is only able to contain about 10 g of soot (if packed loosely). More than 20 g of soot can be fitted into one thimble by extensively pressing during the packing process, although I suspected that the pressing might have negative effect to the releasing of fullerenes by the soot. In this package of work, 22 grams of soot were transferred into thimble B with constant pressing and shaking, while 11 grams of soot were transferred into thimble C with minimum disturbing. Hence I conducted a comparative experiment of extracting fullerenes from thimble B and thimble C.

To summarise, there are 3 goals in this package of work:

1. To confirm the observation of previous work.
2. To study the possibility of simplifying the Soxhlet work by changing the solvent less frequently.
3. To determine the effect of pressing the soot during the packing of thimble.

4.3.2 RESULTS

4.3.2.1 THIMBLE B

In order to mimic the extraction process of the previous experiment, thimble B was extracted in the exact same conditions as the previous experiment, and the schedule of solvent replacement was kept the same as well. The yield for each types of fullerenes from thimble B are recorded in Table 2 below.

Table. 2 The yield for each types of fullerenes from Run 8, thimble 1.

Soxhlet time(hrs)	C_{60} (mg)	Progress(C_{60})	Y@C_{82}	Progress (Y@C_{82})
6	0.47	6%	0.29	13%
12	0.298	10%	0.27	26%
18	0.165	13%	0.22	36%
24	0.321	17%	0.21	46%

30	0.191	20%	0.09	51%
42	0.22	23%	0.15	58%
54	0.395	28%	0.2	67%
66	0.25	31%	0.15	74%
78	0.101	36%	0.04	80%
90	2.51	70%	0.19	89%
102	0.72	79%	0.05	91%
126	0.777	90%	0.11	96%
150	0.5	97%	0.05	98%
174	0.153	100%	0.02	100%

The progresses of extraction of C_{60} and $Y@C_{82}$ were plotted in Figure 7.

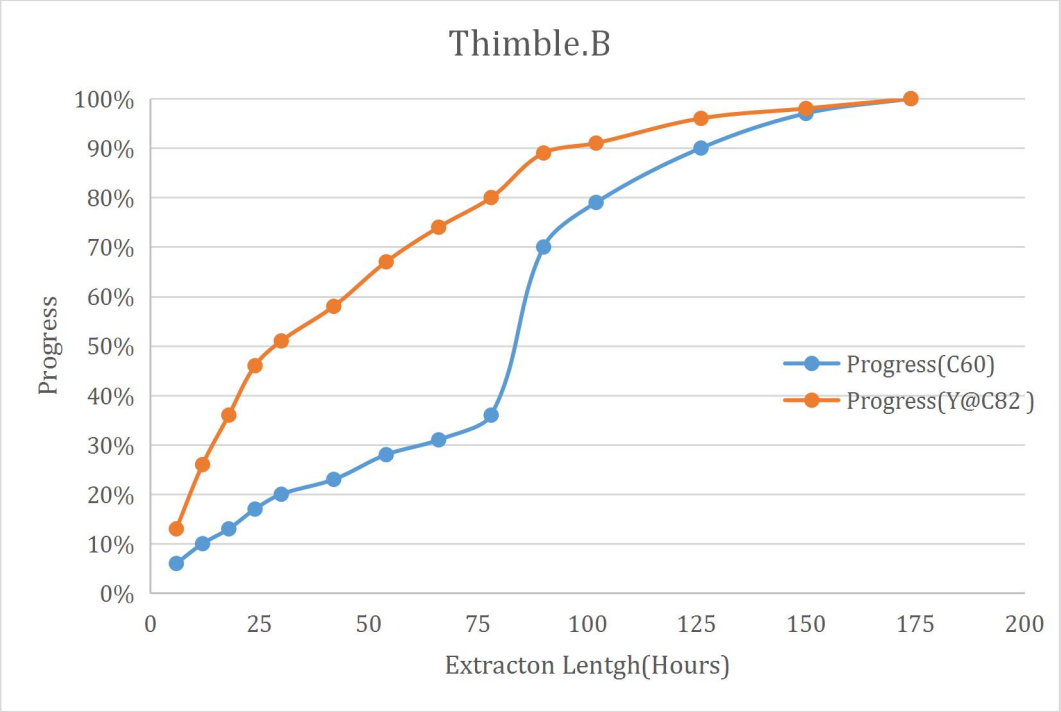


Figure. 7 The progress of the extraction of C_{60} and $Y@C_{82}$ of Thimble B against extraction time.

The progress of extraction of C_{60} was slow for the first 78 hours, a remarkable jump in the yield appeared after the soot had been extraction for 90 hours. The reason for this sudden boost in the yield is unknown.

However, 91% of EMFs can be extracted within 102 hours, and about 80% of C_{60} has been obtain by then, this result being consistent with the previous experiment (95% $Y@C_{82}$ and 85% C_{60} for thimble A) in the same experimental conditions.

4.3.2.2 THIMBLE C

Thimble C was extracted in the same experimental set-up apart from the solvent being replaced every 20 hours. The Soxhlet process was terminated at 100 hours since there was only little fullerene were obtained in 60-80 hours and the yields of fullerenes were extracted in the 80-100 hours slots had already been very hard to read from the HPLC chart. The yield for each type of fullerenes from thimble C are recorded in table 3 below.

Table. 3 The yield for each type of fullerenes from thimble C.

Soxhlet time(h)	C_{60} (mg)	Progress (C_{60})	$Y@C_{82}$ (mg)	Progress ($Y@C_{82}$)
20	0.7665	21%	0.418	42%
40	1.32	56%	0.396	82%
60	1.21	88%	0.162	98%
80	0.24	95%	0.011	99%
100	0.2	100%	0.006	100%

The progresses of extraction of C_{60} and $Y@C_{82}$ of thimble C were plotted in Figure 8.

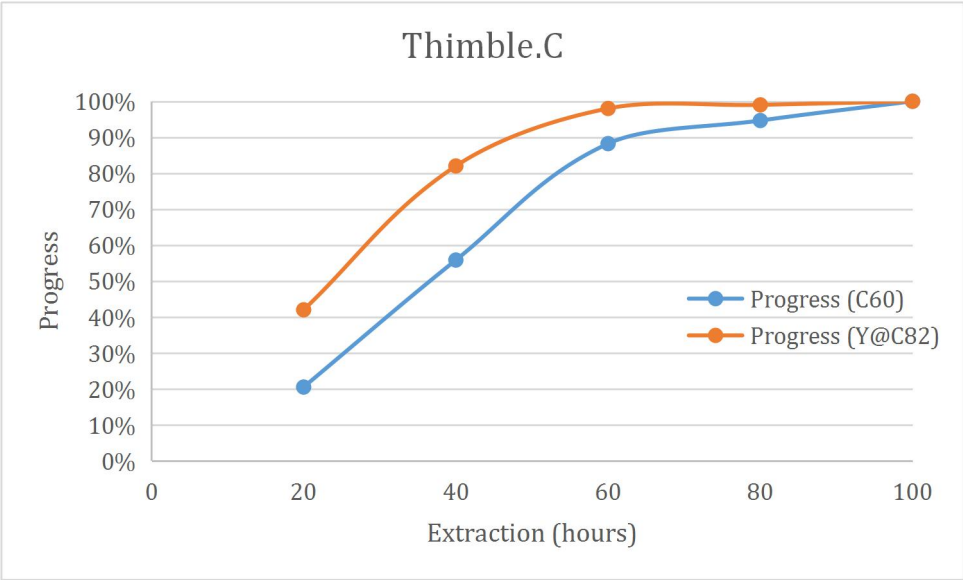


Figure. 8 The progress of the extraction of C_{60} and $Y@C_{82}$ of Thimble.C against extraction length.

4.3.3 DISCUSSION

- The 20 hours-session extraction

Surprisingly, in this run of experiment, more than 90% of both C_{60} and $Y@C_{82}$ came out within 60 hours. The newly scheduled-extraction seems to speed the extraction process up, this may due to the reduction in warming up stage.

- Warming up

It has been seen that no significant amount of fullerenes was released by the soot in the first few cycles of reflux. This is because the Soxhlet was at room temperature as the experiment starts and the fullerenes would only be realized when the solution reached the required temperature. It takes up to 3 hours depending on the frequency of reflux, to warm up the apparatus and the soot to go from room temperature to the required temperature.

- Smoother process

The curves of yield of fullerenes against Soxhlet time are much smoother and regular than their counterpart's in previous experiments, even when compared to the correspondent curves for the first batch of thimble B. It is believed that the longer extraction session evened out the irregularity of the extraction process, and the warming up period is less significant in longer time slots than shorter ones.

- The effect of pressing

By comparing the amount of fullerenes generated from thimble B and C (Table 4), the yields of soot in the two thimbles are very close (thimble B was packed with 22 gram of soot and was expected to releases twice as much as fullerenes than thimble C which contained 11 gram of same quality of soot), the slight difference between the theoretical yields and the actual data could be considered as experimental error. Therefore, there was no obvious negative effect of pressing the soot during packing.

Table.4 The yields of C_{60} and $Y@C_{82}$ from thimble B and thimble C.

	C_{60} (mg)	$Y@C_{82}$ (mg)
Thimble.A	7.36	2.14
Thimble.B	3.74	0.993

4.4 Third Work Package: Soxhlet time optimisation

4.4.1 Introduction

In the last package of work, it was a surprise to observe that the extraction process could be completed within a much shorter length via minimizing the solvent replacement. To confirm the superiority of the 20 hours-session extraction, two more batches of soot were produced as previously described. They were packed into thimble D and thimble E. Thimble D and E were extracted in the same experimental set-up as thimble.C. A pattern of the new extraction scheme is expected to be deduced from this package of work.

4.4.2 Results

The yield of C_{60} and $Y@C_{82}$ from thimble D and E were recorded in Tables 5 and 6, respectively.

Table. 5 The yield of C_{60} and $Y@C_{82}$ from thimble D.

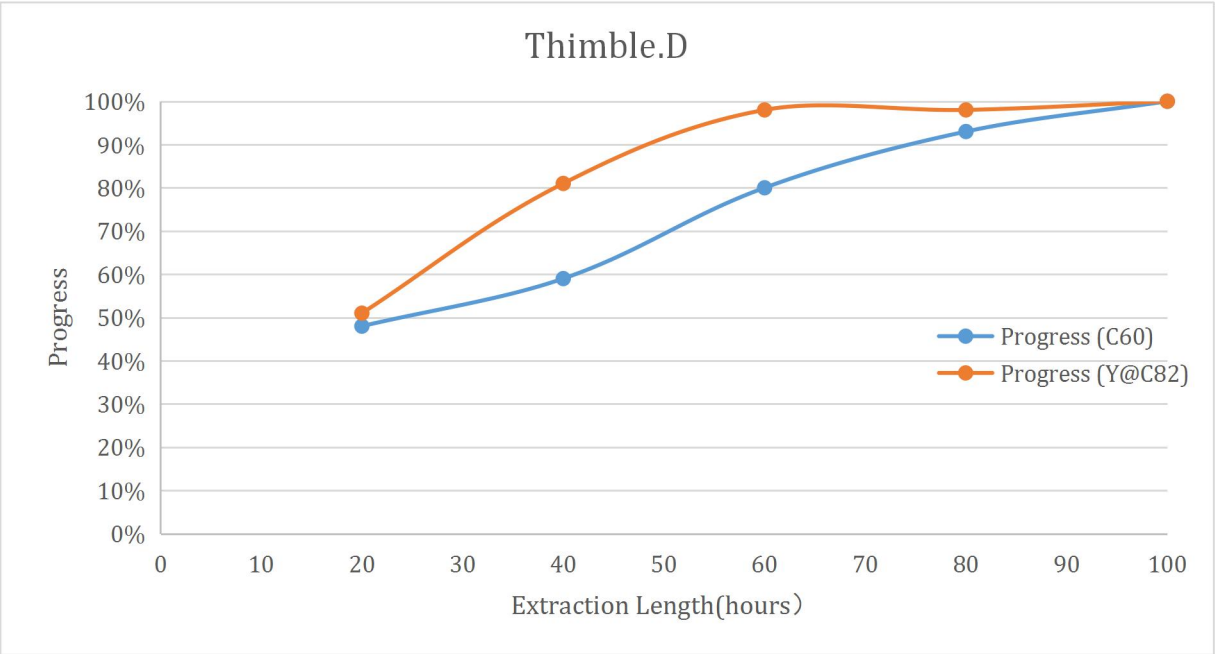
Soxhlet time (hrs)	C_{60} (mg)	Progress (C_{60})	$Y@C_{82}$ (mg)	Progress ($Y@C_{82}$)

20	0.603	48%	0.4587	51%
40	0.132	59%	0.2777	81%
60	0.267	80%	0.1472	98%
80	0.164	93%	0.0080	98%
100	0.083	100%	0.0138	100%

Table. 6 The yield of each types of fullerenes from thimble E.

Soxhlet time (hrs)	C_{60} (mg)	Progress (C_{60})	$Y@C_{82}$ (mg)	Progress ($Y@C_{82}$)
20	18.82	29%	0.4212	43%
40	20.45	60%	0.3241	76%
60	16.54	86%	0.1898	95%
80	6.79	96%	0.0272	98%
100	2.32	100%	0.0176	100%

The progress of the extraction of C_{60} and $Y@C_{82}$ for Thimbles D and E against extraction times were plotted in Figure 9.



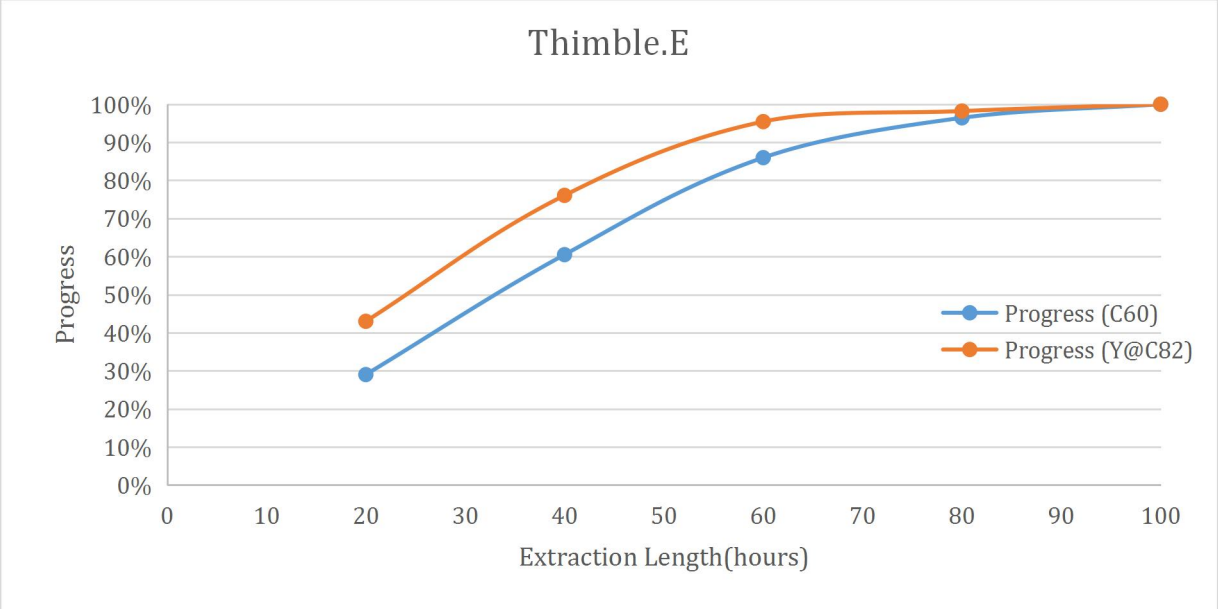


Figure 9. (a) The progress of the extraction of C_{60} and Y@C_{82} of Thimble D against extraction length. (b) The progress of the extraction of C_{60} and Y@C_{82} of Thimble E against extraction length.

4.4.3 DISCUSSION

4.4.3.1 THE DYNAMICS OF SOXHLET METHOD FOR FULLERENE EXTRACTION

Thimbles C and D confirmed the hypothesis that the 20-hours/session extraction is able to extract fullerenes from the soot more efficiently. In fact, it only took 60 hours to extract at least 95% of extractable Y@C_{82}, while more than 80% C_{60} had been extracted by 60 hours as well. Although the progress of the extraction of C_{60} and Y@C_{82} at each measured time-slots had some small variations, a general pattern of the Soxhlet extraction process when the solvent was replaced every 20 hours had been revealed.

Table 7. A comparison of the dynamics of fullerene extraction of thimble C, D and E.

Progress of C_{60}			
Soxhlet Length (h)	Thimble C	Thimble D	Thimble E
20	21%	48%	29%
40	57%	59%	60%
60	91%	80%	86%
80	97%	93%	96%
100	100%	100%	100%

Progress of Y@C_{82}			
Soxhlet Length (h)	Thimble C	Thimble D	Thimble E
20	42%	51%	43%
40	82%	81%	76%
60	98%	98%	95%
80	99%	98%	98%
100	100%	100%	100%

According to Figures 8-9 and Table 7, the yields of EMFs flat out significantly after 60 hours extraction, when at least 95% of EMFs and no less than 80% of C_{60} could be obtained by then. The aim of this project is to improve the efficiency of the generation of $Y@C_{82}$, hence I present that 60 hours will be the optimal extraction length while the solvent can replaced every 20 hours. This optimized Soxhlet extraction scheme has already been adopted by the fullerene production in our lab.

4.5 Conclusions

In this part of the work, I obtained the dynamics of the Soxhlet extraction method for separating fullerenes from the soot. I have also acquired a much better understanding of Soxhlet extraction method.

My main finding has been that empty cages and $Y@C_{82}$ behaved differently in the Soxlet extraction, and the progresses of extraction of $Y@C_{82}$ was always ahead of that of C_{60}. This might be due to the fact that the solvent (DMF) is a polar solvent, which has a high affinity towards the polar EMF molecules.

The suspicion that the pressing of soot during packing has negative effect was not proven to be the case by my experiments. Thus by increasing the soot packing it is possible to process more soot per run.

I found that a Soxhlet extraction process when fresh solvent were replaced every 20 hours led to speeding up the process considerably. This method allowed me to extract 95% of $Y@C_{82}$ from the soot within 60 hours, and a general pattern of this new Soxhlet scheme had been revealed. This scheme had been adopted in our lab to produce various endohedral fullerenes and I believe it is a useful optimization of the EMF extraction process.

5. OPTIMIZATION OF EMF YIELD VIA ARC DISCHARGE

5.1 INTRODUCTION

As mentioned earlier, the production of soot with arc discharge method involves various process parameters, such as helium pressure and discharge current. Part of my project is to determine the most influential variables that affect the yield of EMFs and find out the optimal combination of parameters for generating EMFs.

Due to the nature of the arc-discharge process, the arc current and the helium gas pressure are the most important parameters that are expected to affect the process. Hence I chose to optimize these two parameters. The intensity of direct current sent to generate the arc affects the amount of carbon to be evaporated and the speed by which it does so. The value of the current is usually in a range of 50-500A[35,43]. He gas works as an agent or "atom carrier". The amount of He may affect the way that helium and carbon atoms interact with each other, therefore the yields and the types of products. In the production of fullerenes in our lab, current of 200 amp and 50 mbar He pressure were most commonly used. By considering the capability of the pilot arc discharge system and reviewing the literature,[35,43] high and low values for current were set to 300 amp and 100 amp, respectively. However, when the experiment was conducted, the high current led to the melting of components of the pilot arc discharge system, whereas the low value of current led to very slow burning (which rendered the process impractical), therefore the current used in this experiment was finally assigned to 250 amp and 150 amp as high value and low value. The reference runs were done with 200 amp current and 50 mbar He pressure for comparison.

In order to work out the best yield condition, we need to study not just how each of the variables affect the yield but also how they combine together to affect the yield. To do this, the method "factorial design of experiments" was employed, which is not only able to determine the best yield conditions and the most influential variable, but also demonstrate the combined effect of different variables. Data of yields of fullerenes in various conditions were generated and studied. This work and analysis had been first reported by my co-worker David Barrett in his part II thesis.[41] However, after a better understanding of the dynamics of the Soxhlet was gained, the reported data was realized to be flawed due to insufficient Soxhlet extraction. This work will be introduced in section 5.3. I continued this work by generating the second batch of data (Chapter 5.4). Detailed analysis of this batch of data will be presented in this chapter.

5.2 2^2 FACTORIAL DESIGN

In the 2^2 factorial design, the two variables that will be studied are labeled *A* and *B*. They are set to two different levels, known as high and low levels and usually denoted by a "+" (positive) or "-" (negative) symbol. So in a 2^2 factorial design, we have 4 possible combinations: - - , + - , - + and + +. In this work, the current was labelled as A and He pressure was marked as B.

The effect of A and B are represented by Italic fort of : *A* and *B*.

AB refers to the interaction between A and B. We denote the high level of a variable by the lower case italic letter corresponding to it and a low level of a variable by an omission, so for example, high level of *A* and a low level of *B* would be represented as *a*. the low-low combination would be represented as *1*.

A at the low level of *B* is calculated from [*a*-(*1*)]/n, and *A* at the high level of *B* is given as [*b*-(1)]/n, the main effect of A is calculated form the average of these quantities.

$$A = 1/2n\{[ab-b]+[a-(1)]\}$$

$$= 1/2n[ab+a-b-(1)] \quad (1)$$

Similarly the main effect of B calculated from *B* at the low level of *A* and at the high level of *A*:

$$B = 1/2n\{[ab-a] + [b-(1)]\}$$

$$= 1/2n[ab + b - a - (1)] \quad (2)$$

The interaction effect of AB is given as the average difference between the effect of A at the high level of B and the effect of A at the low level of B:

$$AB = 1/2n\{[ab-b]- [a-(1)]\}$$

$$= 1/2n[ab + (1) -a -b] \quad (3)$$

When the equations for *A* or *B* give a positive value, we say the increasing from the low level to the high level of a certain variable will increase the yield. A positive value for the interaction effect formula suggests that increasing both variables leads to increasing the yield. The magnitude of the value for each equation measures the significance of each variable to the process.

5.3 WORK PACKAGE 1.

5.3.1 EXPERIMENTAL SECTION

The pilot arc discharge system was loaded with 6 carbon rods (10x0.9x0.9 cm) doped with 0.8 % wt yttrium. The system was evacuated to a range from 10^{-5} to 10^{-4} torr by using a vacuum system consisting of a rotary pump backing a diffusion pump. The 6 graphite rods were as described in section. 4.2.1. The collected soot was packed into an extraction thimble which was placed into a Soxhlet apparatus as shown in Figure 3. A. heating mantle was set to level 4.5 (160-170^{o}C) to boil 1 liter of DMF which was evaporated and washed the soot, N_2 gas was used to prevent the soot and solution from oxidation, a magnetic stirrer was span at 500 rpm to stir the solution. The thimble contains the first batch of soot was extracted with DMF in a Soxhlet apparatus for 5 days while the solvent was renewed every 12 hours. The other batches of soot were extracted in Soxhlet for 36 hours while the solvent was replaced every 12 hours. A summary of the burning condition and Soxhlet extraction length of the 6 runs of synthesis of fullerenes were recorded in Table 8.

Table.8 The values of Current and He pressure used in work package 1 and the Sxohlet extraction length of each run of experiments.

	Run.1	Run.2	Run.3	Run.4	Run.5	Run.6
Starting Vacuum (10^{-4} torr)	0.8	6	5	5	4	4
Current (I)	200	150	150	250	250	200
Helium Pressure (mbar)	50	20	80	20	80	50
Soxhlet Extraction time(hrs)	>1 week	36	36	36	36	36

The fullerene-containing DMF solution from each thimble was stirred thoroughly and dried by a Buchi R-200 rotovap and backfilled with Toluene. This procedure was repeated 3 times to ensure a complete removal of DMF. The insoluble impurities found in the processed solution were removed by passing through 0.22 micrometer fluoropore filter paper. The filtered solution was concentrated down by a rotovap. Individual fullerenes were isolated by a JAI LC-9103 HPLC with a Buckyprep-M column (20X250mm), as described in section 4.2.2.3. The area of C_{60}, C_{70}, and Y@C_{82} peaks in the HPLC were recorded and converted into mass by using the calibration formulas that introduced in 4.2.2.

5.3.2 RESULTS

To simplify the discussion, the yield of C_{60} was selected to represent the yields of empty cages (C_{60} is by far the most abundant fullerene molecule). The yields of C_{60} and $Y@C_{82}$ for Runs 1 to 6 are presented in Table 9.

Table 9. *Experimental conditions and yields of C_{60} and $Y@C_{82}$ for Runs 1-6.*

	Run.1	Run.2	Run.3	Run.4	Run.5	Run.6
Starting Vacuum (10^{-4} torr)	0.8	6	5	5	4	4
Current (I)	200	150	150	250	250	200
Helium Pressure (mbar)	50	20	80	20	80	50
Soxhlet Extraction time(hrs)	> 1 week	36	36	36	36	36
C_{60} (mg)	136.9	41	28.4	26.4	30.7	49.3
$Y@C_{82}$ (mg)	15.9	1.55	0.88	1.44	1.68	1.32

5.3.3 DISCUSSION

When Run 1 was carried out, the system was degassed overnight via a pumping system consisting of a rotary pump backing a diffusion pump to $8*10^{-5}$ torr, before the start of the vaporization of the graphite rods, however, since the second run, the system was only degassed to $4\text{-}6*10^{-4}$ torr, it was later discovered that the heating element of the diffusion pump failed since the first experiment and had to be replaced. Nevertheless, a starting vacuum of 10^{-4} torr is well within the range of suitable vacuum for producing fullerenes since the system is consequently flashed with helium during the arc process, so the production of fullerenes (Runs 2-5) continued as planned. The starting vacuum of Runs 2-5 only varies by a small amount, from $4x10^{-4}$ to $6*10^{-4}$ torr. This was the most accurate control of starting vacuum we can get for our system, due to the fact that the arc discharge reactor is a complicated setup involving more than 20 junctions which had to be taken apart, cleaned and re-assembled frequently.

The yields of fullerenes from Run 1 were much higher than the rest of the experiments. Especially the yield of $Y@C_{82}$ from this run was about 10 times than that of the rest of runs. This was thought because the lower starting vacuum of this run. However, when this experiment was repeated after the diffusion pump was fixed, there was no comparable yield increment to be found. Since this experiment was the first arc discharge experiment that my co-worker and I conducted, and other experiments

followed, it is possible that some impurities or other contamination were introduced to the arc discharge system (e.g. residual soot from third-party experiments) when we were conducting the experiment. Another difference between Run 1 and the other 5 runs was that the soot that was generated from the first run was extracted via Soxhlet method for more than1 week, whereas the other batches of soot were only extracted for 36 hours due to time constraints of that specific experiment. Since the result of Run 1 was not reproducible, I decided to exclude this set of data from the quantitative analysis. At the end of this package of work, another set of reference data (Run 6) was generated with 200 amp current and 50 mbar He pressure and the soot was extracted for 36 hours to compensate the data from Run 1. The data of Runs 2-6 were studied, and the analysis was presented in David Barrett's Part II thesis. Since completing the study of the Soxhlet extraction process, I discovered that 36 hours extraction was not enough to separate all the soluble fullerenes from the soot, so it became obvious that the analysis of Runs 2-6 could not accurately reflect the effect and importance of the process. It was however, an excellent basis for building up the study and analysis of the best yield conditions for EMF synthesis.

5.4 Work Package 2.

5.4.1 Introduction

After the first run of EMF production, I continued to work in this direction in order to understand better the best yield condition of arc discharge synthesis of fullerenes and provide useful advice to the production of metallofullerenes, in particular. Another 4 sets of data of yields of fullerenes with different process parameters were generated, while the soot from Run 6 was further processed and the data generated was used as a reference point in this package of work. The details of this work are presented in the following section. When this experiment was designed, an ambitious goal was proposed which was to study the formation mechanism of fullerenes in the arc discharge. The data generated from this package of work would be analyzed for ascertaining how fullerenes and metallofullerenes are formed in the arc discharge. This study will be presented in Chapter 7.

5.4.2 Experimental section

The soot of the previous Runs 1 – 5 had been discarded when this part of the work began; only the soot of Run 6 was kept which had been extracted for 36 hours. The soot was further extracted in the Soxhlet for another 64 hours (100 hours total extraction).

Another four runs of fullerene synthesis in arc discharge were conducted (Runs N1–N4). The soot that was generated from each run was collected and processed the same way as described in work package 1, the only difference was that the soot of the new set of runs was extracted with Soxhlet for 100 hours instead of 36 hours. A summary of the experimental conditions of the 5 runs can be found in Table 9.

Table.9 The values for Current and He pressure used in work package 2 and their respective Soxhlet extraction time for them.

	Run.6	Run.N1 (*1*)	Run.N2 (*a*)	Run.N3 (*b*)	Run.N4 (*ab*)
Starting Vacuum (10^{-4} torr)	4	4	5	4	5
Current (amp)	200	150	250	150	250
He Pressure (mbar)	50	20	20	80	80
Soxhlet Extraction time(hrs)	100				

5.4.3 RESULTS

The yields of fullerenes from each production run were recorded in Table 10.

Table.10 The yields of various types of fullerenes from Run 6 and Runs N1-N4.

	Run.6	Run.N1 (*1*)	Run.N2 (*a*)	Run.N3 (*b*)	Run.N4 (*ab*)
C_{60} (mg)	49.3	102.6	47.4	28.4	15.4
C_{70} (mg)	8.72	40.8	9.5	5.1	2.1
Higher fullerene (mg)	2.8	1.9	2.3	4	3.1
Y@C_{82} (mg)	1.64	0.74	1.94	2.75	2.9

5.4.4 DISCUSSION

The purpose of this work is to maximize the yields of $Y@C_{82}$, so the mass of $Y@C_{82}$ produced from each run was entered into the formulas (1),(2) and (3) .

The main effect of current, *A*, is calculated to be:

$$A = 1/2(1)\{[2.9\text{-}2.75]+[1.94\text{-}(0.74)]\}$$

$$= 0.675$$

Similarly the main effect of He pressure, *B*, is calculated to be:

$$B = 1/2n\{[ab\text{-}a] + [b\ \text{-}(1)]\}$$

$$= 1/2(1)\{2.9\text{-}1.94+2.75\text{-}0.74\} = 1.485$$

The interaction effect of AB, *AB* is calculated to be:

$$AB = 1/2(1)\{2.9\text{-}1.94\text{-}2.75+0.74\}$$

$$= -\ 0.52$$

The positive values of A and B suggest that, as individual variables, both current and Helium pressure have positive effect on the yield of $Y@C_{82}$. On the other hand, a negative value for the interaction effect formula suggests that the combination of high values of current and He pressure has a negative effect to the production of $Y@C_{82}$. This makes for a less clear indication of best values of the variables; however, it is evident that the He pressure has the most significant effect on the yield while the interaction effect was the least important one. Hence I have shown that high He pressure leads to an appreciable increase in the yield of $Y@C_{82}$.

Run.4 is the most confusing experiment among the all. Since *AB* was calculated to be negative and Run.4 produced the most EMFs. I believe this is because the combined effect of *A* and *B*(not the interaction of A and B, but the combined positive influence to the yield of A and B) surpass the negative impact of the interaction of the A and B.

Ideally more data points and for more metallofullerenes would be needed to identify in a finer fashion the "sweet spot" of the interplay between experimental conditions. However this would be a very time consuming project that would go beyond the scope of an MSc programme of research.

5.5 CONCLUSION

Two packages of work were conducted in the search for the best yield conditions for $Y@C_{82}$ with the pilot arc discharge system. However, the first package of work was realized to be flawed after a better understanding of Soxhlet extraction had been obtained. In the second work package, I discovered that both current and Helium pressure have positive effect on the yield of $Y@C_{82}$, on the other hand, the combination of high values of current and He pressure has a negative effect on the production of $Y@C_{82}$. The relationship between the yields and the process parameters are more complicated than I imagined. Nevertheless I was able to show that the yield of $Y@C_{82}$ increased by using high He pressure (80 mbar).

6. A STUDY ON THE FULLERENE FORMATION MECHANISMS IN THE ARC DISCHARGE METHOD

Although fullerenes have been efficiently synthesized by evaporating carbon recourses, the formation mechanism of these materials remains unclear. In this work, we reveal that the formation of fullerenes in arc discharger follows a bottom-up scenario, and endohedral fullerenes (EMFs) are generated by scaling up smaller fullerenes without opening the cages. The validity of two classic formation mechanisms of fullerenes is evaluated.

6.1 INTRODUCTION

Although fullerenes have been discovered more than two decades ago[2], how these molecules are formed from evaporating carbon is still not fully understood. The main reason is that the extreme conditions of synthesis impedes in vivo observation. In searching the literature for the formation mechanisms of fullerenes, both experimental and theoretical studies have been conducted, and numerous formation pathways have been proposed.[16,44,52,53,54,55,56,57] However, I have not found any report on the formation of both empty fullerenes and endohedral fullerenes in the arc discharge method[42], which is one of the most important methods of synthesizing EMFs.

Most formation mechanisms were proposed based on synthesizing empty fullerenes with laser ablation, their applicability in the formation of endohedral fullerenes in the arc discharge method remains unknown. In recent years, more work has been reported on systemizing endohedral fullerenes, these works also provide new clues to reveal the formation puzzle.

After completing the work that was introduced in the previous chapters, I have accumulated a set of data for the yields of fullerenes. A more ambitious goal was set which is to reveal the formation mechanism of fullerenes. The understanding of the fullerene formation mechanism will allow us to improve the yields of fullerenes though ways that were impossible previously. The majority of the published discussion on the formation of fullerenes gives a feeling of “thought experiment”, this is due to the fact that direct observation of the formation of fullerenes in an arc discharge is impossible with current technology. This work is not an exception. Although the discussion is based on our observation of fullerene production, theoretical discussion is also involved.

6.2 DATA

The data were analysed in this study were generated in the experiment that introduced in Chapter 5. In this analysis, these data recorded in Table 10 were rearranged with decreasing yield for C_{60}. The re-ordering is shown in Table 11.

Table. 11 *The yields (mg) of different types of fullerene products from Run 6 and Runs N1-N4. The data is ordered with decreasing yield for* C_{60}.

	C_{60} (mg)	C_{70} (mg)	Higher fullerene (mg)	$Y@C_{82}$ (mg)
Run.N1	102.6	40.8	1.9	0.74
Run.6	49.3	8.72	2.8	1.64
Run.N2	47.4	9.5	2.3	1.94
Run.N3	28.4	5.1	4.0	2.75
Run.N4	15.4	2.1	3.1	2.9

6.3 A REVIEW ON THE CLASSIC FORMATION MECHANISMS

The arc discharge method starts with sending high current though graphite rods, and vaporizes graphite into carbon vapour. [42] Despite the fact that formation of fullerenes via top-down approaches [55,56] has been suggested, isotope studies involving vaporization of graphite containing ^{12}C and ^{13}C have showed that the carbon vapour is made up by small carbon fragments, such as C_2, C_3.[58] (Figure. 11a) These small carbon units are extremely reactive and proceed to form larger clusters immediately.[2]

Beyond that, there are several proposed scenarios on how these clusters evolve into fullerenes. Most formation mechanisms have been disproved by later studies. However, two formation mechanisms are still well-supported and are seen widely as plausible candidates for explaining the formation of fullerenes, namely the “Pentagon road” [52] and the “Fullerene Road”.[59]

6.3.1 PENTAGON ROAD

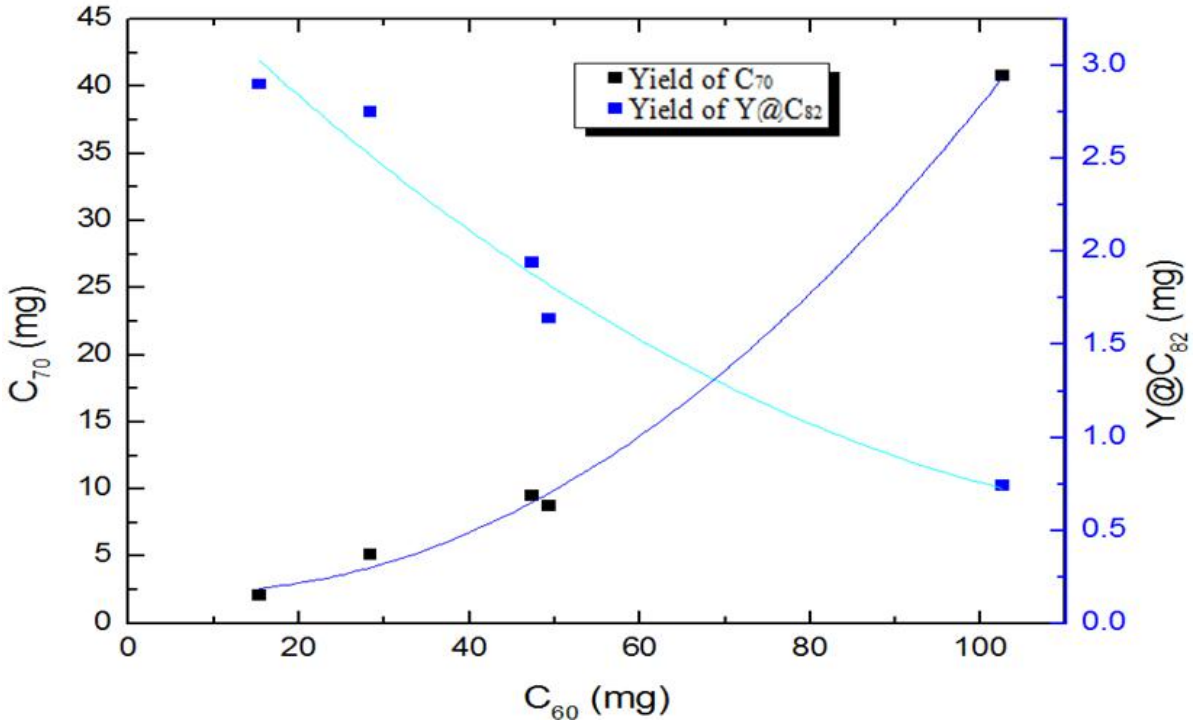
In the year 1992, Smalley[52] and his colleagues synthesized fullerenes with laser vaporization and claimed that C_2, C_3 units come together to form liner chains, which in turn connect to form rings. The formation of polycyclic network led to the incorporation of pentagon and some clusters with the right number of pentagons in proper positions evolve into fullerenes. This scenario is known as "party-line" scheme. In this scheme, fullerene formation of is a very rare event; the majority of carbon sources will end up with gathering as insoluble carbon soot. Later, in order to explain new experimental data that fullerenes could be produced through arc discharge at macroscopic scale, Smalley[16] modified the original "party-line" theory by introducing "pentagon rules", which claims that open graphitic sheet with more than 20 carbon atoms follows 3 rules: 1) it consists solely of hexagons and pentagons; 2) it has as many as pentagon as possible; 3) it will avoid adjacent pentagons. Such structure keeps growing by in-taking more carbon fragments and annealing themselves to satisfy the aforementioned rules until C_{60} is formed. In this scheme, once fullerenes are formed, they do not grow any further as a result of lack of reactive edges.

6.3.2 Fullerene road

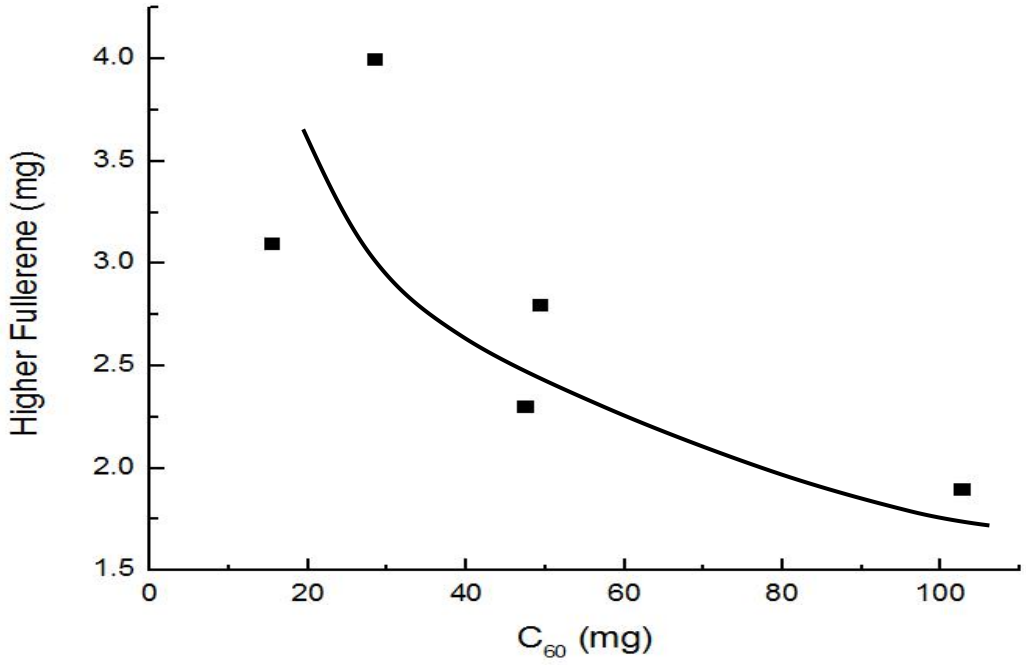
On the other hand, it has been proved both theoretically and experimentally that fullerene is the lowest energy status once a cluster reaches 30-32 carbon atoms. [59,45,60] J.R. Heath[59] proposed a formation scheme different from the "pentagon road" in claiming that clusters adopt the most thermodynamically stable form, i.e. fullerenes, as soon as they reach a critical size (about 30 carbon atoms). In his "fullerene road" scenario, the formation of C_{60} and C_{70} is a result of scaling up small fullerenes by in-taking C_2 and C_3.

6.4 Analysis and Discussion

The fullerenes I produced were characterized by HPLC and mass spectrometry. C_{60}, C_{70}, higher fullerenes and $Y@C_{82}$ are produced in all sets of experiments. The yield of fullerenes bigger than C_{60} including EMF against the yield of C_{60} is plotted in Figure 10 below.



(a)



(b)

Figure 10 (a) indicates that the yield of C_{60} is positively correlated to that of C_{70}. Figure 10 (a) and (b) suggests that there is a reverse relationship between the yields of Yttrium based EMFs and higher empty cages with that of C_{60}.

6.4.1 New fullerene formation scenario for arc discharge method

Despite the two classic fullerene formation scenarios lead to efficient production of fullerenes, neither of them is able to fit my experimental observations. This is discussed below, and a possible fullerene formation scenario, which fits both the experimental observations and theoretical considerations is presented in this discussion.

6.4.1.1 The branching of EMFs and empty cages

The competition between the production of C_{60}/C_{70} and metallofullerenes (Figure 10a) could be explained by the "branching-growth" of production for EMFs and empty cages. In the arc discharge process, small carbon units collide with each other to form bigger units, some clusters managing to capture heteroatoms inside them. The competition between the formation of C_{60}/C_{70} and metallofullerens means that the carbon clusters keep the heteroatoms inside them until eventually they grow into EMFs rather than C_{60}.[57] This means that my observation supports the so called "closed network growth" of EMFs in arc discharge process, where EMFs are formed by scaling up smaller cages that encapsulate metal ions or clusters without opening the cages.[61]

6.4.1.2 The first metallofullerene molecule

By confirming that the formation of fullerenes adopt the "closed cage formation" routine, a question jumps into one's mind, when does the first metallofullerene molecule form?

In the arc discharge process, C_2, C_3 units get together to form clusters. Despite the fact that C_{24} can form a closed cage, C_{32} is the smallest stable cage that could survive the harsh environment of arc discharge process.[45,60,59] It is intuitive to think that the earliest heteroatoms are enclosed by fullerenes is when the cluster has 32 carbons. However, a photodissociation study has shown that carbon shells with metal ions (La+, K+, Cs+) inside them become unstable and break down when the cages shrink to 44-48 members.[60, 7] This experiment implies that a bigger carbon cage (more than 44-48 atoms) is requited in order to accommodate a metal atom. Therefore, I believe that there is a significant amount of clusters that remain as open structures far beyond 32 in size, and the formation of EMFs begins later than that for empty cages. The "fullerene road"[59] claim that when clusters reach the critical size immediately they adopt the fullerene structure is not compatible with my observations.

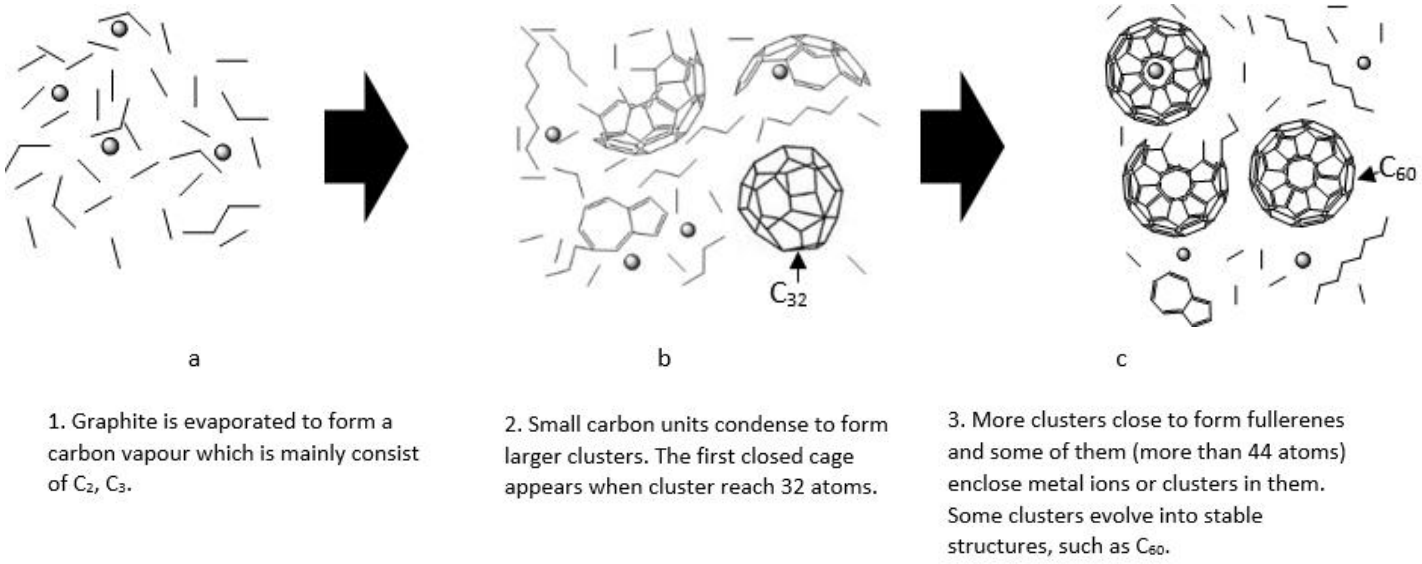


Figure. 11 My proposed simulation of the formation of fullerenes in the arc discharge method.

More recently, fullerenes containing more than one atoms within their empty shell have been synthesized and separated in macroscopic level.[21] A reversed relationship between the yield of Tri-Nitrite fullerenes (TNT) and C_{60} has been seen by Stevenson and his co-workers.[23] This phenomenon has been reproduced by our group (by my co-worker Dr Panos Dallas), which indicates that TNT-type fullerene formation adopts the same route as traditional EMFs， i.e. the closed-growth formation. We can deduce that many clusters stay open even beyond 44-48 carbon atoms in size.

6.4.1.3 THE DOMINANCE OF C_{60} AND C_{70}

Closed carbon cages with/without encapsulating heteroatoms continuously intake carbon fragments to scale up. Eventually, some clusters/cages form C_{60}, which is the first closed cage that satisfies the isolated-pentagon rule (IPR) [52,16]. The remaining open clusters that consist of more than 60 carbon atoms will keep intaking carbon atoms and close later; the next stop for these clusters is C_{70} which is the second structure that obey IPR. It is worth noting that C_{60} and C_{70} are most dominant products initially, newly closed cages with similar size are likely to scramble to form C_{60} andC_{70}.[52,16] C_{60} and C_{70} adopt the same formation path and their similar chemical properties allow them to be produced as the most abundant empty cages and demonstrate a positive correlation (Figure.10a).

6.4.1.4 THE SHIFT IN FORMATION MECHANISM

Figure.10 (b) shows that the behaviour of higher fullerenes is similar to that of $Y@C_{82}$, however, to a less extent. We attribute this phenomenon to a shift in formation mechanisms between smaller cages and bigger ones (including $Y@C_{82}$).

As the process proceeds, less and less Cn (n>60) stay as open structures. Consequently, the closure of open structures to eliminate dangling bonds as a driving force for generating fullerenes becomes less and less significant (Figure.11c). Further lowering of closed cages' energy is mainly achieved by incorporating C_2 units to release the strain, which in turn is responsible for generating higher fullerenes.[62] This scenario is substantially different from the "pentagon road" which claims that closed cages do not grow any further. The shift in formation mechanism also explains the fact that more thermodynamically favoured bigger cages (higher fullerenes) are less abundant than C_{60}, i.e. closed cages are more likely to maintain their state as a consequence of eliminating dangling bonds.

One may argue that the Yttrium ion may go into the cage by re-opening the cage, if this is the case, a competition between the yields of higher fullerene (especially fullerenes that have a size close to the C_{82}) and metallofullerenes should be seen, however, this phenomenon was not observed, instead, higher fullerene and $Y@C_{82}$ demonstrate a similar behaviour.

6.5 CONCLUSIONS

In synthesizing fullerenes with the arc discharge, I have showed that the formation of EMFs involves the "closed-growth network" mechanism. Classic formation scenarios like the "pentagon road" and "fullerene road" are inadequate to explain the synthesis of endohedral fullerenes in the arc discharge method. Based on my observations, I propose that the production of fullerenes by arc discharge method adopts a "bottom up" scenario starting with the condensation of C_2, C_3 units. The precursors of empty cages and EMFs start to appear in the plasma at 32 atoms and more than 44 carbon atoms in size respectively. The "branching-growth" of these clusters lead to a competition between the producing of C_{60}/C_{70} and EMFs. Two main driving forces have been identified in the formation of fullerenes: closure of open structures to eliminate dangling bonds at earlier stage, and scaling up by incorporating C_2 units to release strain energy. The closure of open structures as a formation process leads to a shift in the formation mechanisms. My work provides a possible fullerene formation scenario in

arc discharge method, and a stepping-stone to fully understand the formation of fullerenes. This work may also open new opportunities to tune the distribution of fullerenes products in arc discharge method.

7. POSSIBLE MODIFICATIONS OF THE ARC DISCHARGE SYSTEM

7.1 INTRODUCTION

The purpose of the pilot arc discharge system is to produce small quantities of fullerenes for the lab use and test the patented concept of burning multi-rods in each run,[40] but the ultimate goal is to develop a novel arc discharge system that is able to provide sufficient materials for scientific exploration of fullerenes and beyond (e.g. commercial use). During carrying out experiments with the pilot arc discharge system, I gained insight into the arc discharge method of making fullerenes and a good understating of the pilot arc discharge system itself. I believe that the production of fullerenes can be significantly increased by modifying the design of the current system.

The problems of the current system has been identified and will be discussed in this chapter, followed by the possible approaches to solve these issues and optimize the pilot system. Finally, a new design of arc discharge system which is able to address these issues and to improve efficiency and safety will be presented.

7.2 IDENTIFIED ISSUES

The issues associated with the current system have been identified as follows:

1. Long degassing time

Once the production of fullerene is completed, the arc discharge system is taken apart in order to collect the soot and after charging the system with new rods, the apparatus is reassembled. To degas the reassembled system to the desired vacuum, takes at least 12 hours. This time is almost as long as the fullerene production process itself if not even longer.

2. Loss of soot during the manual collection procedure. Potential exposure of personnel to carbon nanomaterials

The soot collection process requires a person to brush the soot off the wall of the arc discharge chamber and collect it though the gas outlet which is at the bottom of the chamber. The soot is made of very fine carbon particles, which contain nanomaterials. The soot can disperse in the air during the collection process; it had been noticed that the table next to the pilot system was covered by soot after soot collection. This

dispersion leads to loss of materials, but most importantly, the person who conducts the experiment can get exposed to nanomaterials.

3. Insufficient cooling of some components vulnerable to heat/high current.

The heat generated when passing high current to the graphite rods to create a plasma would be conducted to the chamber of the arc discharge by the diffusion of hot soot and He gas, hence sufficient cooling of the chamber is needed. The chamber of the arc reactor is cooled via a water-filled copper tube welded on the chamber walls. This system worked but not as effectively as one would have hoped. Passing water in the tube did remove the heat away from the reactor surface but the chamber is only partially covered by the copper pipe. The areas that were not water-cooled warmed up rapidly and reached 200^{o}C within 1 min during the arc operation. The process had to be stopped to prevent overheating, and it normally took 5 mins for the system to cool down to a temperature low enough that operation could be resumed.

In addition, it had been found that the copper plate and shaft were prone to melting when 300 Amp current was used to vaporize the rod. This limited our system to operating with current < 300 A, although high current had been found to be in favour of $Y@C_{82}$ production. The PTFE screws on the copper plate would melt with almost every single run while the PTFE plate used to block the soot from entering the feedthrough mechanism melted several times.

Last but not the least, the arc discharge system contains more than 20 junctions, ranging from welded junctions to O-ring based junctions. This is the reason why it was not possible to cover the entire surface of the chamber with cooling water pipe. The lack of sufficient cooling led to many junctions undergoing a number of expansion/shrinking cycles during the operation. This could lead potentially to poor vacuum inside the chamber over time and reduce the life of the system.

4. Loss of soot through the pumping system

The rods that were used in this project were produced by Toyo Tanso ltd. The average weight of each rod was measured at about 13 grams. We usually “burn” 70% of the rod to avoid damage the copper plate that holds the rod in place, in theory, the burning process should be able to generate 13*70%*6 = 54.6 grams of soot, however, we are only able to recover about 30 gram of soot.

There are 3 sources of losing materials:

1. The loss of materials during the soot collection process (this issue has been discussed earlier).

2. The main chamber of the arc discharge system was directly connected to the pumping system. I found that the oil of the diffusion and rotary pump was black and muddy, which indicated that soot had been sucked through the pumps.

3. The rods are doped with metal oxide. It is possible that the oxide releases oxygen at high temperature, which combines with carbon to produce carbon monoxide or carbon dioxide which in turn is pumped out from the system. The loss of materials by reaction with oxygen is unavoidable but attempts were made to minimize the first two sources of soot loss.

7.3 Modification of the synthesis of fullerenes process with the pilot system

To address these issues, attempts to modify the pilot system have been made. Solutions to some of the identified issues that had been adopted/tested are discussed in this section.

7.3.1 Hoover soot collection

The soot is typically collected manually by the operator. Although PPE are used (such as mask and goggles) the skin can still be exposed to nanomaterials. In order to minimize the exposure of personnel to the nanomaterials, a vacuum hoover equipped with a HEPA-approved filter was purchased and used to collect the soot from the arc discharge system in collaboration with the University safety office. The vacuum hoover removed the soot from the wall of chamber efficiently, however, it had been found that some soot got stuck to the hoover filter and only 50% of the soot could be recovered even after extensive brushing of the filter.

7.3.2 The integration of a vacuum filter

The loss of soot into the pumping system not only leads to loss of hard-obtained soot, but also causes contamination of the pumping system. A vacuum filter was purchased and placed between the main chamber where fullerenes were produced and the pumping system. There was a risk that the soot might block the filter and result in pressure building up in the chamber, however, no such issue was encountered during the operation. After burning 6 rods, the tube that connects the filter to the pumping system was found to be clean, which meant that there was no soot escaping from the

filter and into the pumps. The soot trapped by the filter was weighed to be about 5 grams, which corresponds to one sixth of the total soot that could be collected from the chamber. This has proved to be a very efficient method for increasing soot production and maintaining a clean pumping system and has been employed ever since.

7.3.3 Attempts to improve the cooling system

The sides of the main arc reactor became hotter gradually since they had no cooling system attached to them. I installed new water-filled cooling plates (that we purchased for this purpose) on the sides of the reactor, However, the adhesive for the cooling plates failed at elevated temperatures, therefore I abandoned this solution and I had to resort to the original configuration with the existing cooling system.

7.4 New generation of arc discharge system

The patented idea of burning multi-rods in each run of arc discharge production of fullerenes had proved to be effective. However, the pilot system is not able to fully exploit the potential of this design. A scaled up system will be built to satisfy the both scientific and commercial demand for fullerenes.

A new design of arc discharge system that has the potential to avoid the identified issues associated with our pilot system and that is able to produce soot safely and more efficiently is suggested here. A schematic show of the new design of arc discharge system is presented in Figure 12.

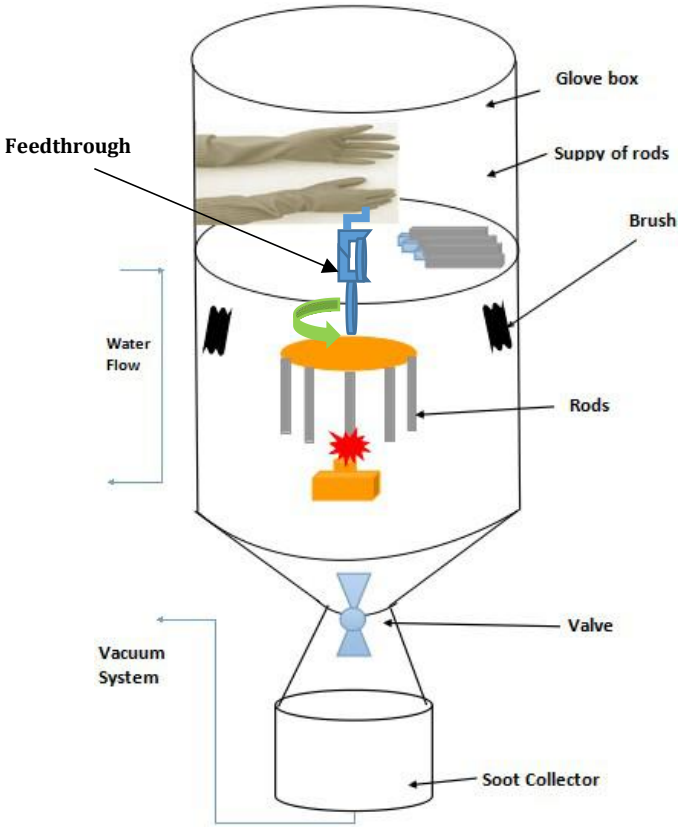


Figure. 12 New design for arc discharge system

Concepts that are integrated into the new designs are discussed below. The new system consists of 3 sections: a glovebox, a main chamber and a soot collection chamber. The glovebox and the main chamber are separated by a gas-tight door, while the collection chamber is isolated from the main chamber by a valve.

- New method for rod recharging:

A glovebox is integrated at the top of the reactor. It allows the recharging of the graphite rods to be completed under inert gas environment. To ease the rod recharge process, an easy switch device will be employed instead of the original friction-based fixing method to keep each rod in place. This new approach allows the charging of rods to be performed without introducing air, therefore, the degassing process (issue 1) could be minimized.

The feedthrough system that attached to the pilot arc discharge system has been proved to be an effective method of moving forward the rod and rotate it. The same concept is adopted in the new design. A more ambitious design is to integrate sensors to monitor the burning and automate the production of soot.

- Novel pressure-difference driven soot collecting method:

In the new design, a brush is fitted into the interior wall of the chamber, this brush can be moved up/down to swipe the soot away from the wall of the chamber. A soot collector is connected to the main chamber and isolated by a valve. Once the soot is swiped off the wall, a pressure difference can be created between the two chambers by filling the main chamber with He or N_2 gas while the valve remains closed. Once a certain pressure is reached, the valve is opened, a downward gas flow is generated which brings the soot into the collection chamber. This process can be repeated until the all the soot is sucked into the collection chamber. This new soot collection method can eliminate the manual soot collection process, which exposes personnel to nanomaterials and can minimise the soot that is lost to the air. By combining the glovebox and the novel soot collection method, the entire soot generation process can be performed without opening the system; productivity can be improved considerably.

- Improved cooling system and replacing the high temperature/current components:

The running of the current system has to be stopped every 1 min to prevent overheating as a result of lack of sufficient cooling system. The main chamber of the new version system is double-walled which allows water to pass through it to take the heat away during the operation and relieve it from thermal expansion/shrinking cycles. As mentioned before, some components are vulnerable to the high temperature, e.g. copper plate and shaft, PTFE components. If the burning process can be continued non-stop, these components are expected to maintain a good performance under extreme temperature, so new materials like superalloys (e.g. Ni-alloy) will be employed to manufacture the key components of the system.

- Improved sealing method to increase the lifetime of the system:

Although all junctions are cleaned carefully, the vacuum of the pilot system tends to deteriorate over time. In the current system, several junctions are only about 10-15 cm away from the heat source, which has a temperature as high as 2000-2500^{o}C during operation. The thermal expansion/shrinking cycles at these junctions are harmful. To prevent the same problem happening to the new system, the numbers of junctions of the system will be reduced.

7.5 CONCLUSIONS

In this chapter, we discussed the issues that slow down the production of fullerenes with the pilot arc discharge system and potential hazards that are associated with the current soot collection method.

The 4 major areas that need to be improved are: very long degassing times, the inefficiency of the soot collection method, vulnerability to the heat, and soot into the pumping system. Modifications to the pilot arc discharge system have been made already. The integration of vacuum filter effectively prevents the soot entering the pumping system and additional soot can be collected by the filter. The novel design of arc discharge system that I am suggesting is able to produce soot continuously, safely, and more easily.

8. $TiCl_4$ BASED EMF PURIFICATION METHOD

8.1 INTRODUCTION

My project involves the optimization of the production of EMFs. One of the most important stages during EMF production is their purification. To date the most widely used method is HPLC. HPLC works very effectively for the production of high purity samples. However it is a tedious and very labour intensive process. Currently HPLC is the time controlling stage for EMF production. At the same time it is a factor that limits the generation of EMFs.

It has been reported that Lewis acids preferentially react with tri-metallic nitride templated fullerenes (TNTs) and oxometallic fullerenes (OMTs) to form insoluble complexes, which can be separated from other empty cages by filtration.[39] Akiyama and co-workers reported that the same separation method can be applied to metallofullerenes Mx@Cn (M = metal; x = 1,2; n >70) and carbide metallofullerenes of the $MC_2@C_{n-2}$ (y = 2,3,4; n-2 >68) type.[1] The separation/purification is controlled by the oxidation potential of the starting materials, species with first oxidation potential lower than 0.62-0.72 V vs Fc/Fc+(e.g. $Y@C_{82}$) react with the Lewis acid readily and can be effectively separated/purified form the empty cages. According to some recent reports, among all the Lewis acids, $TiCl_4$ was found to be the most efficient candidate to purify EMFs and a recovery rate of 100% had been achieved.[1,63] In this chapter I have ascertained the possibility of integrating $TiCl_4$ separation scheme into our metallofullerenes production process.

8.2 EXPERIMENTAL SECTION

About 30 g of soot containing Yttrium based-EMFs and empty cages were produced as descried in 4.2.1.1. The newly developed 20 hours-session Soxhlet scheme(with 2L of DMF) was employed to extract fullerne from the soot, and the total extraction length was 80 hrs.

The extract was dried by a Buchi R-200 rotovap and 100 ml toluene was added to dissolve the precipitate. 2 ml of the resulting solution was taken by a syringe and injected into a JAI LC-9103 HPLC for examination. Calibration formulas(F.1) that introduced in 4.2.2 were used to convert the HPLC chart to the masses of different species of fullerenes, the result would be used as a reference.

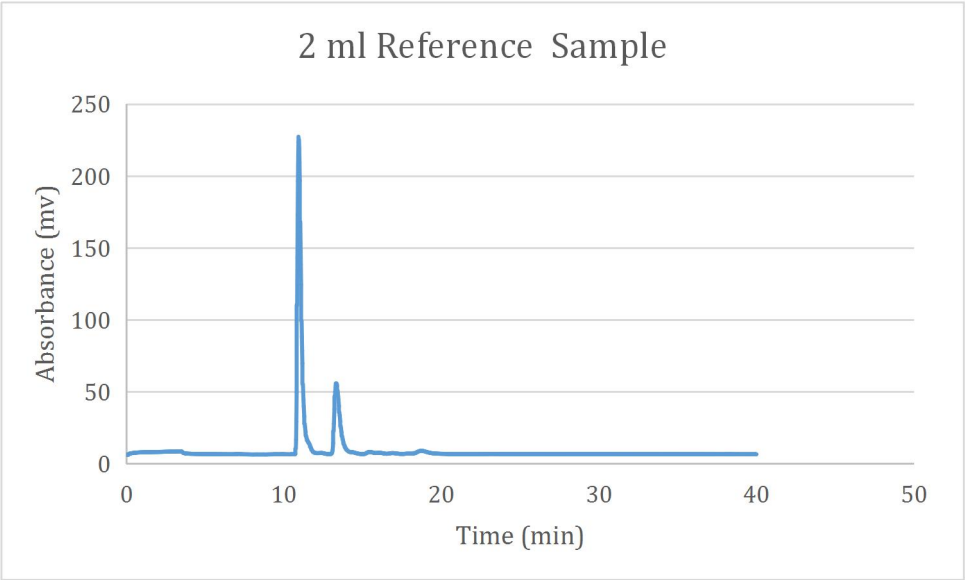
Another 5 ml of solution was taken and added to a test tube, 1 dose of $TiCl_4$ was added to it and stirred until a precipitate appeared. Once the precipitate stopped forming, the cloudy solution was passed through a PTFE membrane (0.22 micrometre, omnipore, Merck Millipore) to remove the precipitate. The filter paper, which was covered by brown precipitate was washed by plenty of distilled water to remove any metal halides formed. 2 ml of acetone was applied to remove the excess water. The acetone-washed filter paper was immersed into 50ml toluene and sonnicated to reclaim the EMFs. The experiment was repeated with various reaction times and different solvents (CS_2).

Experiments were also performed with $AlCl_3$ and $CuCl_2$. In these cases, 0.5 mg of $AlCl_3$ or 0.43mg of $CuCl_2$ was added to 5 ml of solution and stirred. After 2 min of reaction time, the solution was passed though a PTFE memebrane (0.22 micrometre, omnipore, Merck Millipore) to remove the precipitate and excessive Lewis acids. The filter paper was washed by distilled water to completely remove the Lewis acids, and 2 ml of acetone was used to remove the excess water. The acetone-washed filter paper was immersed into 50 ml toluene and sonnicated to reclaim the EMFs.

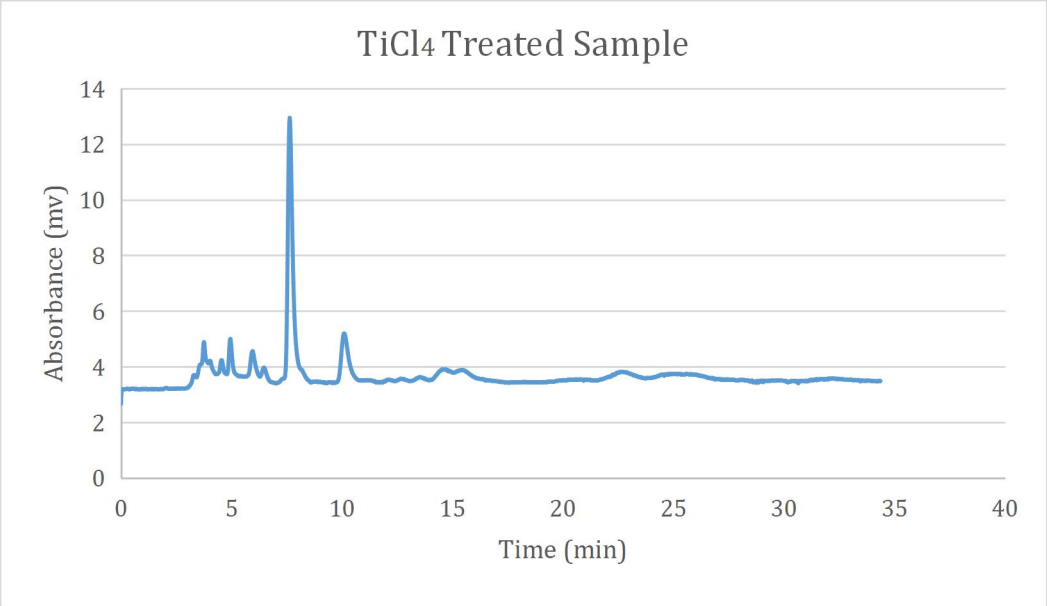
The solutions that contains reclaimed materials were concentrated and characterized by HPLC and F.1 was used to convert the HPLC chart to the masses of fullerenes.

8.3 RESULTS

About 97-99% of C_{60}/C_{70} and 85-92% of higher fullerenes can be removed from the soot, however, the amount of $Y@C_{82}$ that was reclaimed was lower than expected, and the highest recovery rate of $Y@C_{82}$ was about 67%. The HPLC result of the 2 ml starting materials and the $TiCl_4$ treated sample of this experiment is presented in Figure 13 (a) and (b). The amount of various fullerenes species present in the sample is recorded in Table 12. According to Table 12, 98.4% of the C_{60} and 98.6% of C_{70} were removed by the treatment. The residual higher fullerenes in the $TiCl_4$ treated sample was much higher, which represents 10.7% of that in the starting materials. Approximately 67% of the $Y@C_{82}$ was recovered after the $TiCl_4$ treatment.



(a)



(b)

Figure. 13 The HPLC chart of the 2 ml starting material (a) and the $TiCl_4$ treated sample (b).

Table12. The composition of the reference sample, the 5ml starting material and the $TiCl_4$ treated sample.

	C_{60}(mg)	C_{70}(mg)	Higher fullerenes(mg)	Y@C_{82} (mg)
Reference (2ml)	0.9690	0.2800	0.0400	0.0052
5 ml Starting Materials	2.4225	0.7000	0.1000	0.0129
Lewis Acid Treated 5ml	0.0390	0.0097	0.0107	0.0086
Recovery rate	1.6%	1.4%	10.7%	66.7%

Recovery rate is defined as the ratio of each species of fullerene present in the Lewis acid treated solution against the starting materials. For example, the recovery rate of Y@C_{82} was calculated as follows: 0.0086 mg / 0.0129 mg = 66.7 %

8.4 Discussion

8.4.1 Residual higher fullerenes

By employing the $TiCl_4$ separation method, more than 98% of C_{60} and C_{70} and about 90% of higher fullerenes can be removed from the soot within 10 mins, further improvement in separation efficiency might be achieved by improving the operation of the experiment.

However, no complete removal of higher fullerenes was seen in any of the trials. This is because bigger cages have lower oxidation potential; empty cages that consist of 90 carbon atoms or more possess oxidation potentials lower than 0.5-0.6 V vs. Fc/Fc+, and they form a complex with $TiCl_4$ along with Y@C_{82}.[39] We know that bigger cages such as C_{90} were produced as by-products along with Y@C_{82} in our arc discharge synthesis, therefore it was not surprise to see that there was a certain amount of higher fullerenes in the $TiCl_4$ treated sample. It seems that there is no effective way to avoid the production of bigger cages and so the complete removal of higher fullerenes with $TiCl_4$ seems unattainable at the moment.

8.4.2 The recovery rate of Y@C_{82}

The highest recovery rate that had been achieved in this part of the work was 67%, which was lower than expected, based on previous literature. The possible reasons for the low recovery rate are discussed below.

8.4.2.1 The decomposition of $TiCl_4$-Y@C_{82} complex

One obvious possibility for the low recovery rate is that the crude solution was lost during the operation. For this reason, the recovery rate of C_{60} and C_{70} was studied. The solution that passed thought the filter paper was examined by HPLC. It was found that the solution contains 97-98% of the starting C_{60} and C_{70}, which means that there was no loss of crude solution during the operation. However, I noticed that there was a certain amount of Y@C_{82} present in the solution that passed through the filter paper; the amount of Y@C_{82} was calculated to be 10% of that in the starting material. I believe that this material was introduced into the solution by decomposition of a $TiCl_4$-Y@C_{82} complex during the filtration process(Scheme.1).

$$TiCl_4 + Y@C_{82} \longrightarrow [TiCl4]^-_m [Y@C82]^+$$

$$[TiCl4]^-_m [Y@C82]^+ \xrightarrow{H_2O} HCl + Ti(OH)_4 + Y@C_{82}$$

Scheme. 1

The solution was exposed to air during the filtration, $TiCl_4$-EMFs complex decomposed as $TiCl_4$ reacted with water vapour in the air, it is worth noting that $TiCl_4$ is extremely reactive with air. When this experiment was conducted in a fume hood, a large amount of white/yellow fume was created once $TiCl_4$ was removed from the rubber-sealed bottle. Once the complex was removed, Y@C_{82} was released back into solution, which passed through the filter paper.

Following this, the water and acetone that was used to wash the filter paper were examined. The water/acetone used to wash the filter paper were dried in a rotary evaporator, and toluene was added to dissolve any soluble materials in the flask. The new solution appeared to be light yellow. By injecting this sample into HPLC, I found that a small amount of Y@C_{82}, which corresponds to 3-4 % of the starting material was in the sample. Adding the material that was reclaimed from the filtered solution and water/acetone to the material that was recovered from the filter paper, it amounts to about 80% of the Y@C_{82} in the starting material. This is significant but still falls short of the total Y@C_{82} in the starting material.

8.4.2.2 Unstable Yttrium cation

One possible reason for the 20 % loss of Y@C_{82} is the formation of unstable cation [Y@C_{82}]+ during the experiment. During the reaction, Y@C_{82} transfers one electron to

the $TiCl_4$ to form $[Y@C_{82}]+$, which is a notoriously unstable cation. It reacts with water and oxygen to form hydroxylated derivatives and oxide.[64]

8.4.2.3 REACTION TIME

The precipitate started to form after 1 min of adding $TiCl_4$, and stopped growing after 2 mins. I wondered how the reaction time affects the recovery rate of $Y@C_{82}$. Therefore, after adding $TiCl_4$, the resulting solution was tested after 2min (5 runs), 5 min (5 runs), 10 min (5 runs), 30 min (3 runs), 60 min (3 runs) and 120 hours (1 run). It appears that the recovery rate of $Y@C_{82}$ decreases as the reaction time increases, and there was no $Y@C_{82}$ that could be reclaimed when the solution was exposed to air for 60 hours or more. The average recovery rate (calculated from $[X_1+X_2...X_5]/5$) of samples that were tested are recorded in Table 13 and plotted in Figure 14**.**

Table 13. The (average) recovery rate of $Y@C_{82}$ at various reaction times

Reaction time (min)	Average Recovery rate of $Y@C_{82}$
2	50%
5	40%
10	23%
30	5%
60	0%

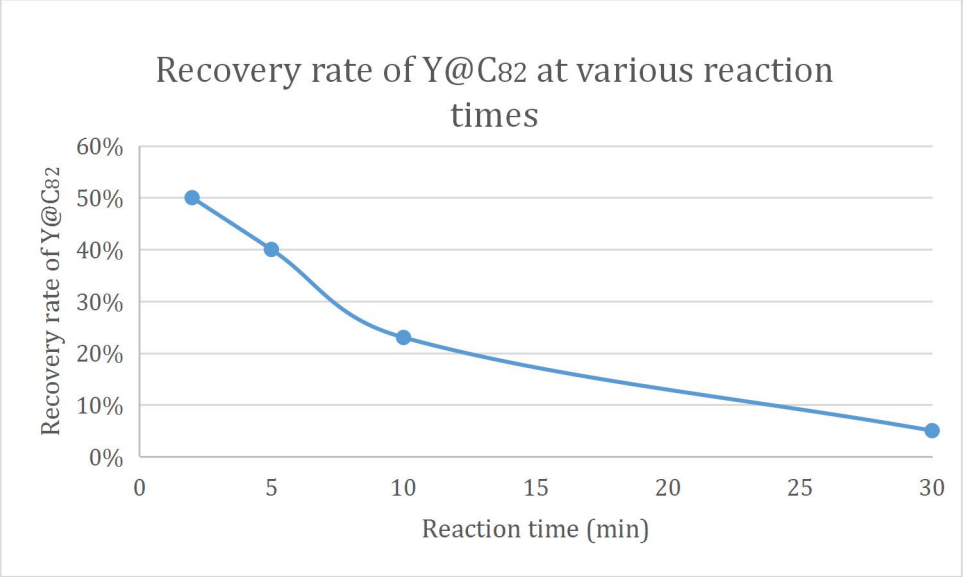


Figure. 14 The recovery rate of Y@C_{82} in various reaction time

The highest recovery rates were achieved when the solution was filtered once the precipitate stopped growing, and about 50% of the starting Y@C_{82} could be reclaimed. The recovery rate decreased as the reaction time increases, and the recovery rate fell to zero when the solution was exposed to air for 60 hours or more. I believe this is because of the decomposition of the $TiCl_4$-Y@C_{82} complex and the oxidation of the metallofullerene. One $TiCl_4$ treated sample was left in the fume hood for 24 hours, the cloudy solution became very light yellow and transparent, while a brown jelly-like phase appeared at the bottom of the test tube. The light yellow solution was injected into HPLC for testing but there was no metallofullerenes signal that could be seen in the resulting HPLC chart. The yellow colour of the solution might come from the hydroxylated or oxidised Y@C_{82}.[64]

8.4.3 The influence of solvents and types of Lewis acids

$TiCl_4$ separation was performed in various solvents, in addition to toluene. Experiments with CS_2 and DMF were also conducted, and it seems that the efficiency and recovery rate of Y@C_{82} was independent of the solvent. Separations with different Lewis acids ($CuCl_2$ and $AlCl_3$) also were conducted, however, there was no higher efficiency on either recovery rate or amount of separation that could be seen in these experiments.

8.4.4 General discussion

The efficiency of $TiCl_4$ separation may be improved by conducting the experiment under the protection of inert gas, e.g. in a glovebox. However, this was not possible in our lab. By considering the recovery rate of $Y@C_{82}$, this method is not recommended to be integrated into the EMFs generation process for the reasons summarized in the following paragraph.

8.5 Conclusions

In this chapter I described efforts into using a Lewis acid, especially $TiCl_4$ to separate $Y@C_{82}$ from empty cages. However, the efficiency of this method was not as good as expected. Although the selectivity of Lewis acids had been proved to be good, the high recovery rate of EMF that had been reported by other labs were not reproduced in our lab. The highest recovery rate of $Y@C_{82}$ that was achieved in this project was 67% (that could be extended up to 80%). I believe the main reason for the lower recovery rate was because the decomposition of the $TiCl_4$-EMF complex and the degradation of the $Y@C_{82}$ cation.

I found that the recovery rate decreases as the reaction time increases, and the recovery rate falls to zero when the solution is exposed to air for 60 hours or more. Separation with various solvents and Lewis acids were conducted, but no better separation scheme was found.

Hence I conclude that, for $Y@C_{82}$ at least, the use of carefully controlled environment such as a glove box is necessary for separation using Lewis acids. Therefore I cannot recommend it to be integrated into the EMFs generation process in our lab.

However, an method that is able to efficiently separate EMFs from the empty cages during the Soxhlet stage was developed in this project, this separation method is introduced in the next Chapter.

9. TWO-STAGE SOXHLET SEPARATION METHOD

9.1 INTRODUCTION

In this chapter I developed a two-stage Soxhlet extraction method and employed it to extract and purify EMFs/TNTs from the soot. In the first stage, toluene was used to separate more than 99.5% of C_{60}, C_{70} and higher fullerenes from the soot. The solvent is switched to DMF in the second stage where more than 95% of EMF/TNT can be obtained within 40 hours further Soxhlet extraction. This is an efficient, simple and scalable method for separating/purifying EMFs/TNTs from the soot. I aimed at submitting this work for publication however, I discovered that the application of the similar concept to La and Y based mono-EMFs had already been reported.[65] Nonetheless, this method is efficient and speeds up the production of EMFs considerably by significantly reducing the dependence on tedious and laborious HPLC process. For this reason this is an integral piece of my effort to optimize the whole process of EMF production and I am describing it in the following sections.

9.2 EXPERIMENTAL SECTION

In order to produce mono-metallofullerenes and TNTs, the pilot arc discharge system was recharged with 6 graphite rods containing 0.8%wt Yttrium oxide, which were drilled and packed with 10%wt $Cu(NO)_3$. These rods were burned with same procedures as descried in Section.4.2.1.1 in Chapter.4, the experimental conditions were 50mbar He, 200 amp current.

After rod vaporization, the soot was collected and packed into one extraction thimble. This thimble was washed with toluene for 40 hours while the solvent was renewed every 20 hours. A magnetic stirrer span at 500 rpm to stir the solution in the flask. The resulting solution was filtered by a filter paper (0.22 micrometer, Fluoropore) to remove any impurities. The filtered solution was named *Toluene-extract*.

In the second stage, the toluene-washed thimble was dried in a fume hood, the Soxhlet extraction was continued with DMF for another 4 sessions while each session lasted for 20 hours. The resulting solution was dried by a rotavap and backfilled with Toluene, these procedures were repeated 3 times to ensure complete removal of DMF. Again, the processed solution was passed through a filter paper (0.22 micrometer, Fluoropore) to remove any impurities. The filtered solution was named *DMF-extract*. Both stage.1 and stage.2 were performed under the protection of a N_2 atmosphere. The

Toluene-extract and DMF extract were analysed by a JAI LC-9103 HPLC equipped with a Buckyprep-M column (20X250mm).

9.3 RESULTS

The production of empty fullerenes and EMFs/TNTs ($Y@C_{82}$ and $Y_3N@C_{80}$) were confirmed by MALDI-mass spectrometry (Figure 15). The results of HPLC examination of the *Toluene-extract* and *DMF-extract* are shown in Figure 16. The contents of the *Toluene-extract* and *DMF-extract* are presented in Table 14.

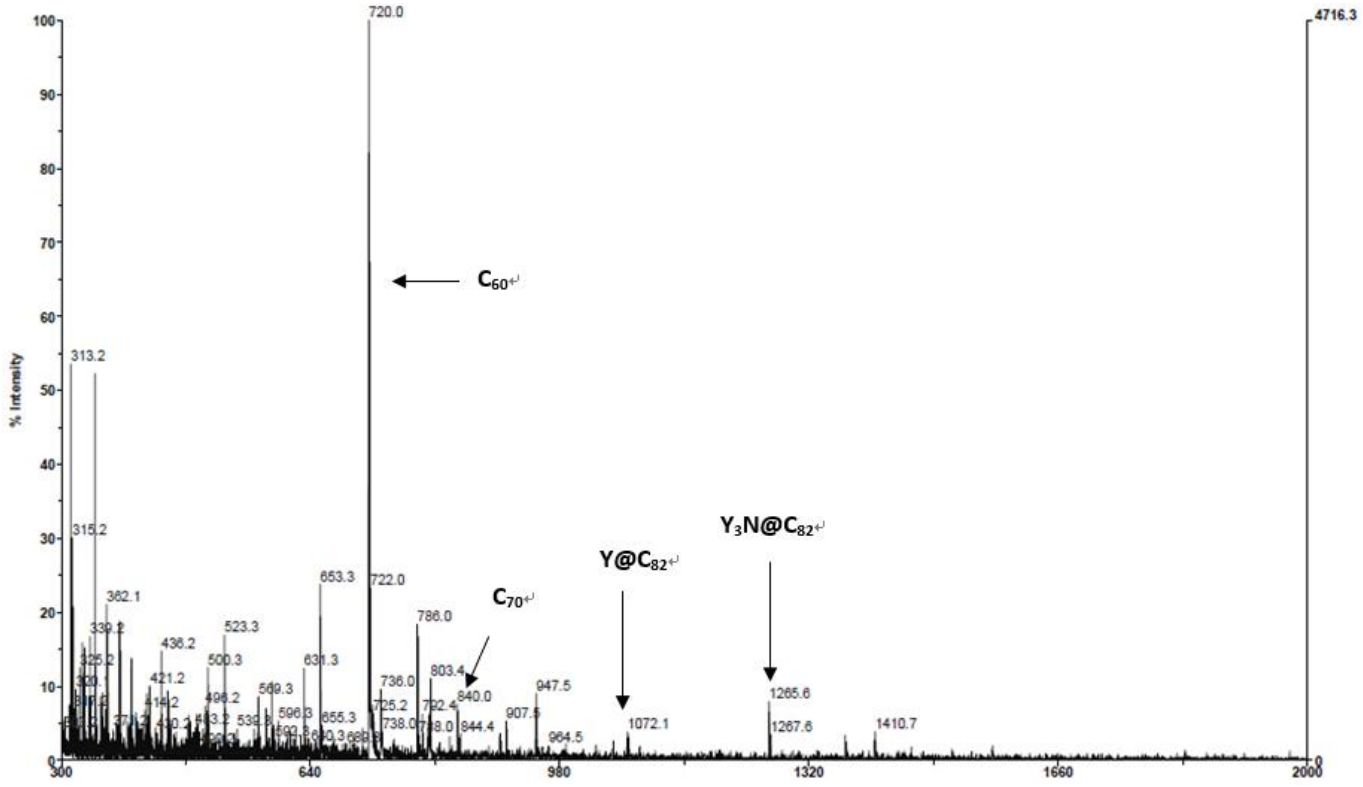
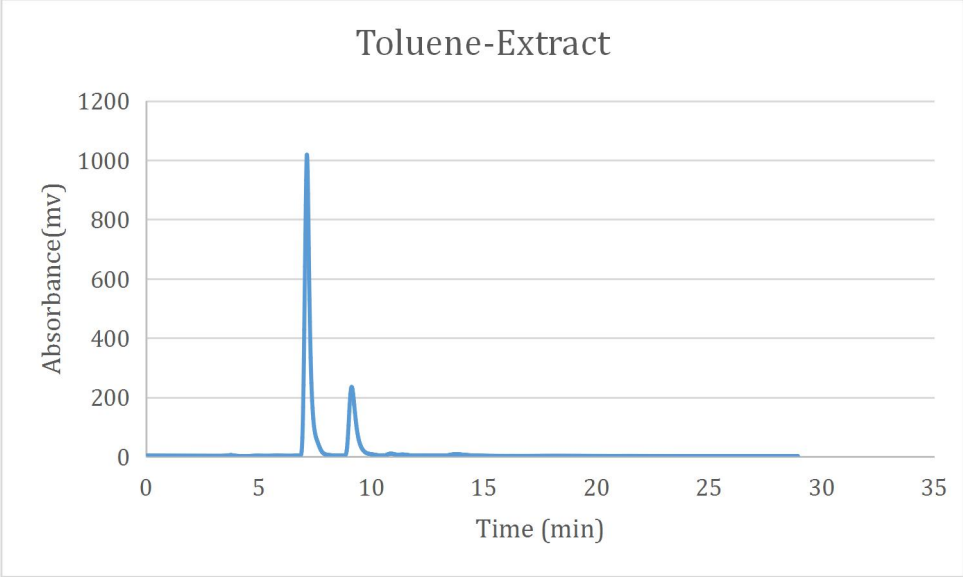
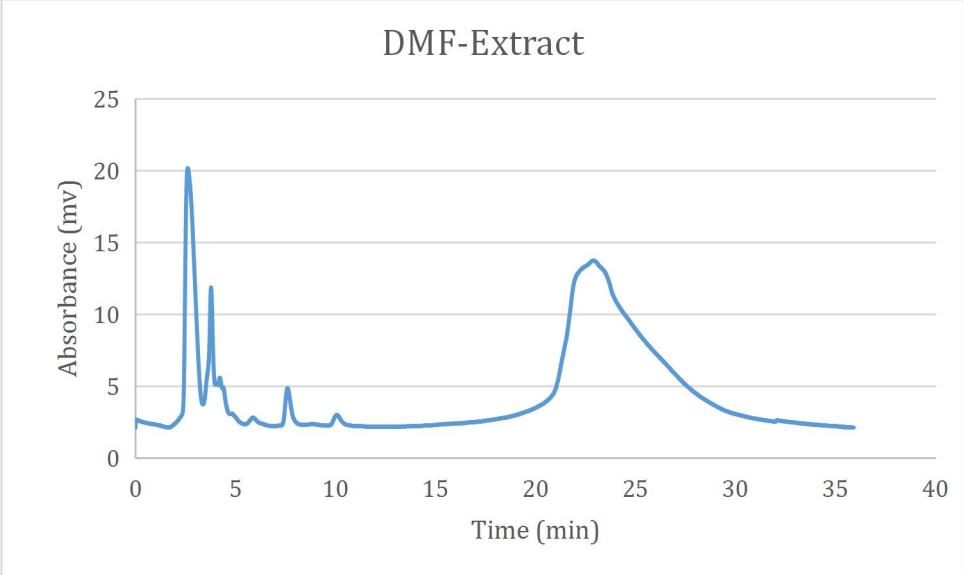


Figure 15. The MALDI-mass spectrum of the soot (Mass spectra were recorder at the National Mass Spectrometry Facility at Swansea).



(a)



(b)

Figure 16. HPLC examination of the toluene-extract (a) and DMF-extract (b).

Table 14. Contents of the Toluene-extract and DMF-extract (values in mg).

	C_{60}	C_{70}	Higher Fullerene	$Y@C_{82}$ & $Y_3N@C_{82}$
Toluene Extract	19.863	5.5388	0.5435	0.01041
DMF Extract	0.025	0.009	Nil	1.216

Total	19.888	5.5478	0.5435	1.226
Toluene Extract/Total	99.87%	99.84%	100%	0.85%
DMF Extract/Total	0.126%	0.16%	/	99.15%

9.4 DISCUSSION

More than 99.8% of C_{60}, C_{70} and higher fullerenes were obtained from stage 1, whereas 1.226 mg of EMF/TNT were extracted from the second stage which corresponds to 99.15% of the total amount of EMF/TNT that had been separated from this batch of soot. There was no measureable higher fullerene signal in the DMF extract. There was less than 1% of EMFs/TNTs removed from the soot in stage 1. This amount of material was not recovered.

The DMF extract contains EMFs/TNTs with a purity:

[$Y@C_{82}$ & $Y_3N@C_{82}$] / [C_{60}+C_{70}+Higher Fullerenes+$Y@C_{82}$ & $Y_3N@C_{82}$] = 1.216 /(0.025 + 0.009 + 1.216)= 97.3%

9.4.1 THE DYNAMICS OF THE TWO-STAGE SOXHLET METHOD

The soot was washed by toluene for 40 hours (done in 2 sessions, 20 hours each) and then extracted with DMF for 80 hours (done in 4 sessions, 20 hours each). I discovered that the colour of the solution that was obtained from the 3rd and 4th DMF extraction sessions was rather light. After examining the resulting solution with HPLC, the 3rd DMF extraction session generated about 4% EMF, and the 4th DMF extraction did not produce any measurable EMFS/TNTs. This means that 95% of EMFs/TNTs can be separated from the soot within 40 hours DMF extraction (the 1% loss of EMFs/TNTs in stage 1 has been taken into account). This EMFs/TNTs releasing rate is higher than expected. In the study of the dynamics of the traditional DMF Soxhlet extraction process, we have learnt that it takes 60 hours to extract more than 95% EMFs from the soot. The reason for the higher extraction rate of EMFs/TNT in the two-stage Soxhlet method might be due to the fact the toluene acts as a first solvating agent for the soot, therefore it can be extracted more readily in DMF. Another possible explanation is that the presence of $Cu(NO)_3$ during rod vaporization alters the morphology of the soot which facilitates the releasing of EMFs/TNTs during the Soxhlet extraction. However, the two-stage Soxhlet

extraction/purification seems to work similarly for both pure metal-oxide rods and Cu-doped rods.

9.4.2 The integration of the two-stage Soxhlet extraction method

Soxhlet extraction of fullerenes from the soot is a necessary step in the process of obtaining EMFs/TNTs. The separation/purification of EMFs/TNTs in this stage considerably reduces dependence on the tedious, laborious and expensive HPLC process.

In the traditional fullerene generation process, the soot was extracted with DMF in Soxhlet, the resulting solution was filtered and concentrated down for purification with HPLC which is a very time consuming and laborious work. In the HPLC purification stage, 2 to 2.5 ml of fullerene-containing solution is injected into the HPLC every time, and it takes about 30 mins for the solution to travel though the columm and the fullerenes to be separated into each individual species. During this process, a person is required to monitor the progress of separation and to collect the fractions of solution that contain different fullerene species. Unwanted solution is also collected which needs to be distilled to recover the solvent. By considering the fact that each arc discharge run is able to generate 50-150 ml of raw soot solution (filtered fullerene-containing solution), the HPLC purification stage takes one person to work in full capacity from 3 days up to 1 week.

By employing the two-stage Soxhlet extraction/purification method, the EMFs and TNTs have been purified to more than 97% purity. This separation efficiency is comparable with the HPLC method. However, even in this case, HPLC is required to separate $Y@C_{82}$ and $Y_3N@C_{82}$. When Yttrium oxide doped rods were brunt to produce $Y@C_{82}$, the desired species can be obtained in high purity with minimal use of HPLC. This new method takes 80 hours (40 hours toluene extracton + 40 hours DMF extracton) to obtain 95% of the EMFs/TNTs, compared to the traditional one stage Soxhlet extraction which takes 60 hours to separate at least same amount of EMFs from the soot. But the longer extraction time can be compensated by the reduction in the HPLC time, and the Soxhlet extraction does not need a person's constant attention.

9.4.3 The origin of the separation/purification with the two-stage Sohxlet method

The success of the two-stage Soxhlet came from the fact that a non-polar solvent (such as toluene, o-xylene) and a polar solvent (such as DMF) were used to extracted

fullerenes with different dipole moments, i.e. EMFs and TNTs possess larger dipole moments than empty cages due to the fact that they have asymmetrical electronic structure,[65] which in turn is caused by their distorted cages and encapsulated metal ions.[66]

The efficiency and reliability of this modified Soxhlet extraction/purification method has been confirmed by my colleague Dr Panos Dallas who employed this method to extract/purify various endohedral fullerenes from the soot. So far, this method has been successfully applied to separate: Y, Gd, Ho, Er based EMFs and TNTs from empty cages. In a previously published report, o-xylene was used instead of toluene. This solvent has a solubility of C_{60} even higher than that of toluene, [67] and DMF was employed to extract EMFs in the second stage.[65] The two-stage Soxhlet extraction with the combination of o-xylene and DMF might be a useful combination in future work.

9.5 Conclusion

Y@C_{82} and TNT-type fullerene $Y_3N@C_{80}$ were produced in this experiment. A two-stage Soxhlet extraction/purification method has been developed independently in our lab. This method allows more than 99.8% of C_{60}, C_{70} and higher fullerenes to be removed from the soot in the first stage during which toluene was used as the solvent and 95% of EMFs/TNTs could be obtained after extracting the soot with DMF for another 40 hours. The extracted EMFs/TNTs have purity of more than 97%, which is good enough for most work. In any case, HPLC can be further used if needed to increase sample purity.

Although I discovered that this modified Soxhlet extraction/purification method was previously reported by another research group[65], the integration of this new approach simplifies and speeds up the generation of EMFs considerably and is therefore an integral part of my research project.

10. OTHER COMPLIMENTARY ACTIVITIES

In addition to pursuing the main goal of this project, which is to scale up the arc discharge synthesis of EMFs, other activities were also performed. In this chapter I describe experiments that did not relate to the main objective of this project but produced encouraging results that might lead to future work.

10.1 TRIALS OF SYNTHESIZING NOVEL ENDOHEDRAL FULLERENES

10.1.1 THE DIVERSITY OF ENDOHEDRAL FULLERENES

Endohedral fullerenes can be divided into two classes, endohedral metallofullerenes and endohedral non-metallic fullerenes. The latter group of endohedral fullerenes is more recently discovered. Saunders et al[68],[69] reported the synthesis of He@C_{60} and Ne@C_{60}, since then, more noble gas atoms and other non-metallic elements have been put into the fullerene cavity.[26,70] More recently, fullerene cages containing non-metallic compounds, such as: HeN@C_{60} and HeN@C_{70}, have been made and the result has been confirmed by X-ray diffraction analysis.[71]

In this project, I focused on EMFs. EMFs can be divided into 3 groups based on the encapsulated species, they are: mono-EMFs, di-EMFs, and cluster-EMFs. A mono-EMF has only one metal atom in its carbon cage. The first recognised EMF La-fullerenes belongs to this family.[3] Although more and more mono-EMFs have been synthesized, there is no report on encapsulating transition metals together with noble metals inside fullerenes, these elements' outstanding catalytic ability is considered to disable the forming of fullerene cages.[11] For most of the mono-EMFs, the encapsulated metal atom donates 2 or 3 electrons to the carbon cage. Fullerenes that have two guest metal atoms inside them are known as Di-EMFs. EMFs with than three pure metal atoms have not been identified yet. But species formed by combining metallic elements and non-metallic atoms have been widely made, these metallic clusters include: carbide, nitride, oxide, sulfide, cyanide etc.[11]

The first Nitride cluster EMFs were reported by Dorn and his co-workers in 1999.[37] This formation of new fullerene species started with an accidental leakage. Air was introduced and as a result, Sc_3N moiety was formed and trapped by C_{80} cage. Soon after the first nitride EMF has been confirmed, Sinohara et al synthesized the first carbide EMF:Sc_2C_2@Cx[72]. The formation of this new type of fullerene was supported by NMR

and synchrotron radiation powder diffraction coupled with Rietveld treatment of the diffraction data and maximum entropy method analysis methods (SRPD/Rietveld/MEM).[72] Subsequently, metal oxide EMFs and metal sulphide EMFs were synthesized by introducing a small amount of elemental oxygen or sulfur into the fullerene making system. [38,73] Although hundreds of fullerene species have been discovered and synthesised to date, the discovery of new endohedral fullerenes are stilled reported regularly.

10.1.2 Synthetic Strategy

The production of fullerenes was performed by burning graphite rods doped with a mixture of metal oxides and solid nitrogen resources, to produce novel bi-metal fullerenes, TNTs and carbide EMFs.

The ability of burning multi-rods in each run with the pilot arc discharge system was the main advantage. Rods with different doping combinations were used with 200 Amp current in the presence of 50mbar He gas.

The details of the doping were summarized below:

- Formula 1

  Base Rods：2.0% Nd/graphite rod

  Doping:

  1%La_2O_3

  1%La_2O_3+10%$Cu(NO_3)_2$

- Fomula 2
  Base Rods: 2.0% Nd/graphite rod
  Doping:

  1% Y_2O_3

  1% TiO_2

  1% Y_2O_3 + 10% $Cu(NO_3)_2$

1% TiO_2 + 10% $Cu(NO_3)_2$

- Formula 3
  Base Rods: 2.0%Ho/graphite rod
  Doping:

  1% Y_2O_3

  1% Gd_2O_3

  1% Er2O3

  1% Y_2O_3 + 10% $Cu(NO_3)_2$

  1% Gd_2O_3 + 10% $Cu(NO_3)_2$

  1% Er_2O_3 + 10% $Cu(NO_3)_2$

- Formula 4
  Base Rods: 0.8%Ho/graphite rod
  Doping:

  2% Y_2O_3

  2% Gd_2O_3

  2% Er_2O_3

  2% Y_2O_3 + 10% $Cu(NO_3)_2$

  2% Gd_2O_3 + 10% $Cu(NO_3)_2$

  2% Er_2O_3 + 10% $Cu(NO_3)_2$

10.1.2.1 The suppression of the catalytic effect of Fe by copper

Fe has been known to benefit the formation of nanotubes and impede the production of fullerenes, whereas Cu was believed to increase the yields of fullerenes.[74] In this part of the work, graphite/iron oxide composite was filled with $Cu(NO_3)_2$ and pure copper to impede the catalytic effect of iron in the hope of producing Fe-based endohedral fullerenes.

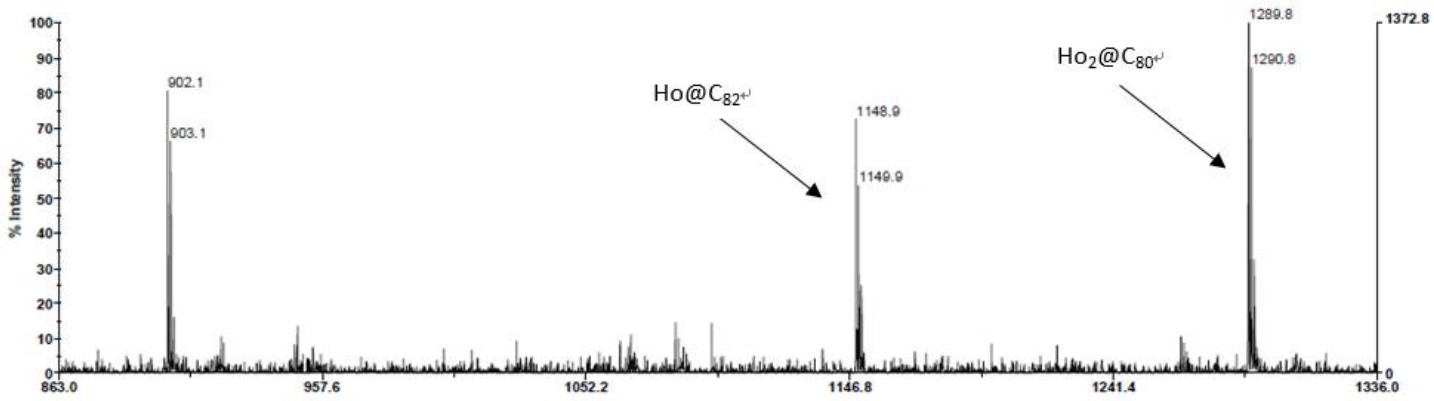
10.1.3 RESULTS & DISCUSSION

12 runs of the arc discharge synthesis were carried out, however, in this section, only the production of rare fullerene and observations and findings that might lead to the discovery of new EMFs and are presented and discussed.

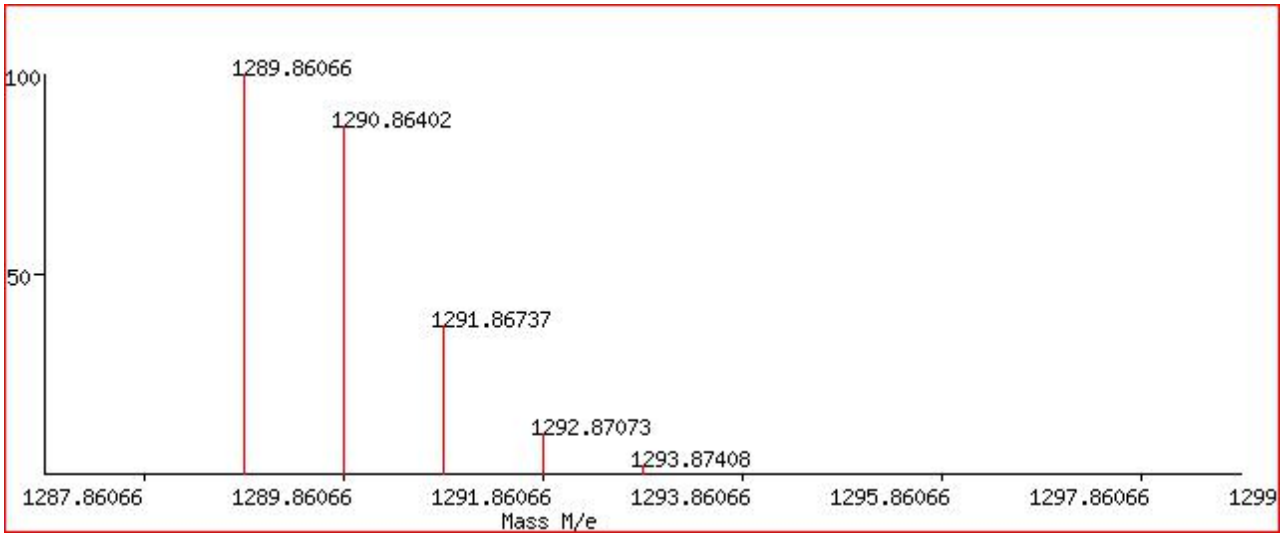
10.1.3.1 Ho_2+C_{80} ENCAPSULATED FULLERENE

When Holmium doped rods were burnt, a rarely seen $Ho_2@C_{80}$ (or $Ho_2C_2@C_{78}$) was found to be produced in relatively high abundance based on mass spectrommetry (Figure 17). This molecule was only mentioned by an article in a very general way and no clear signal of $Ho_2@C_{80}$ is shown in the reported mass spectrum chart.

It is worth noting that although the possibility that this signal represents Ho-based endohedral fullerenes was very high, the structure of this molecule is unknown. Further study is required to ascertain the details of this molecule. For example, a UV-VIS study should be able to distinguish that the molecule consists of a C_{78} or C_{80} cages by studying its absorbance. If the molecule was proved to adopt a carbide endohedral fullerene structure, the novelty and scientific value of this discovery will be very higher and this could lead to a useful publication.



(a)



(b)

Figure 17. (a) The mass spectrum of $Ho_2@C_{80}$ (or $Ho_2C_2@C_{78}$) produced by NMSF; (b) Predicted mass spectrum of $Ho_2@C_{80}$($Ho_2C_2@C_{78}$)

10.1.3.2 Fe + C_{60}

The soot generated by burning copper filled Fe rods was tested by HPLC and MALDI.

A small bump could be seen at around 20 min of the HPLC chart (Figure. 18), where the EMF signal usually appears. The fractions that came out the HPLC before 20 min and after 20 min were collected by two flasks and sent for mass spectrum analysis. The mass spectrum of these two samples were shown in Figure 19 (a) and (b).

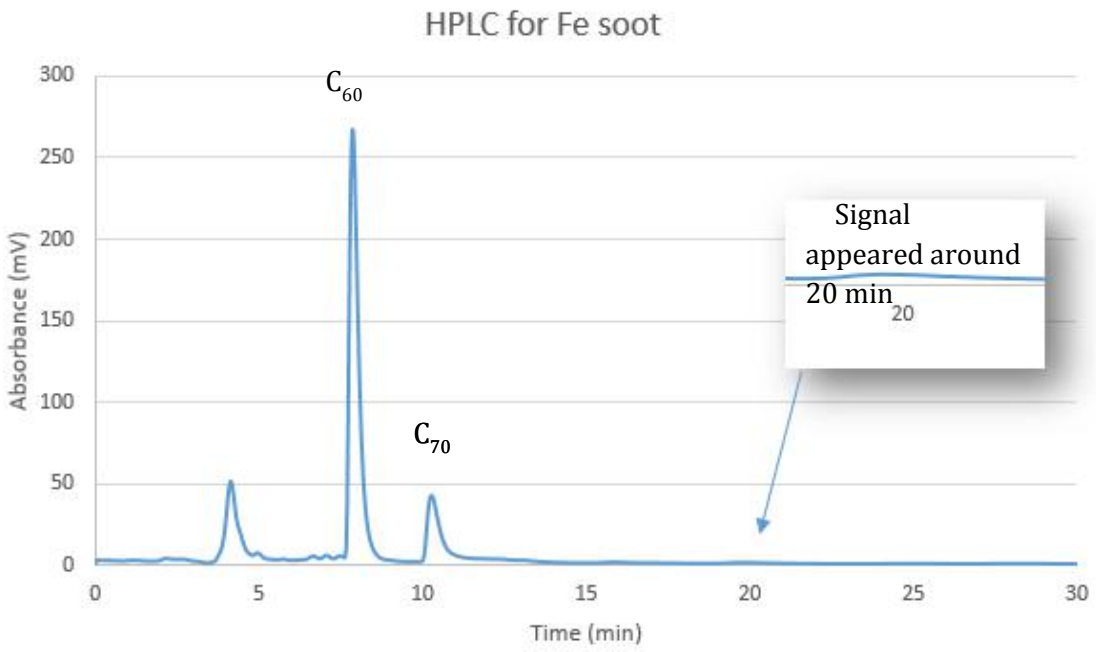
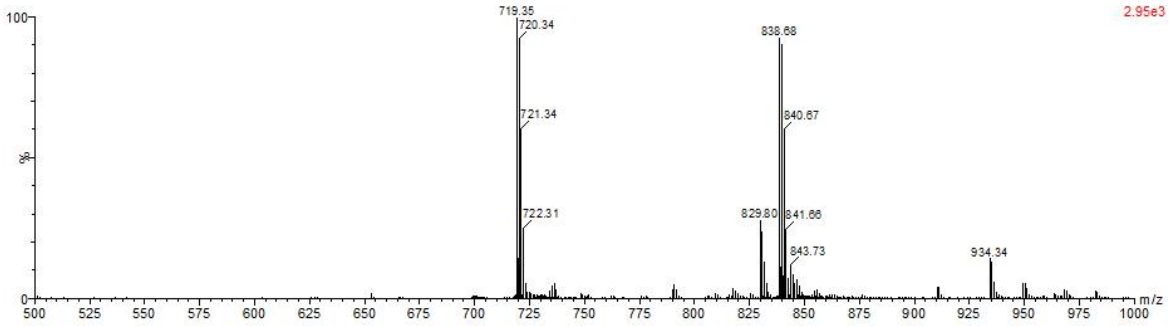
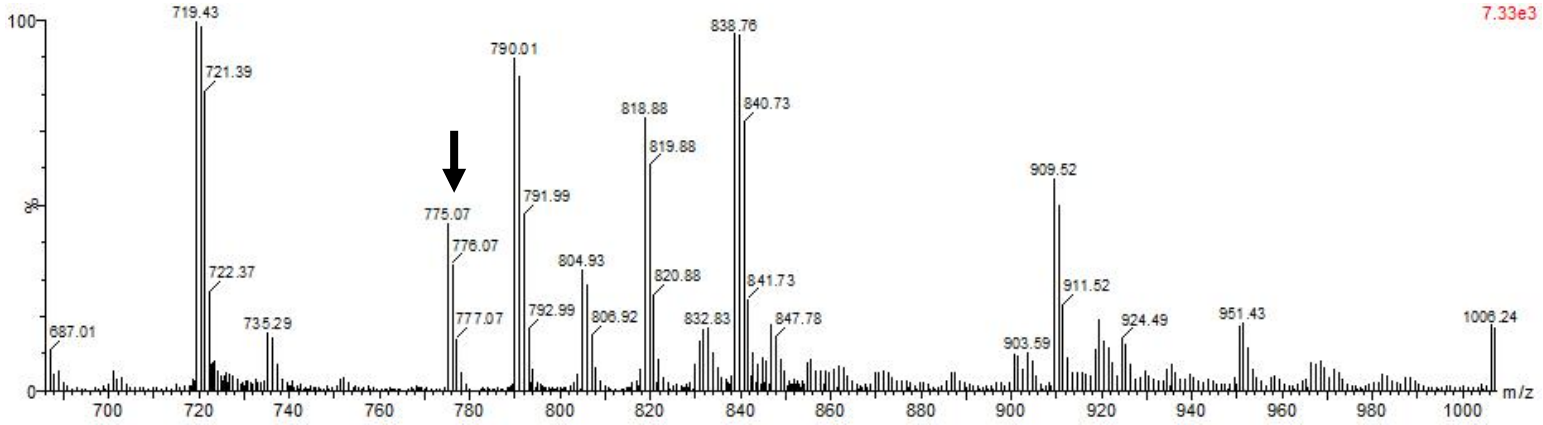


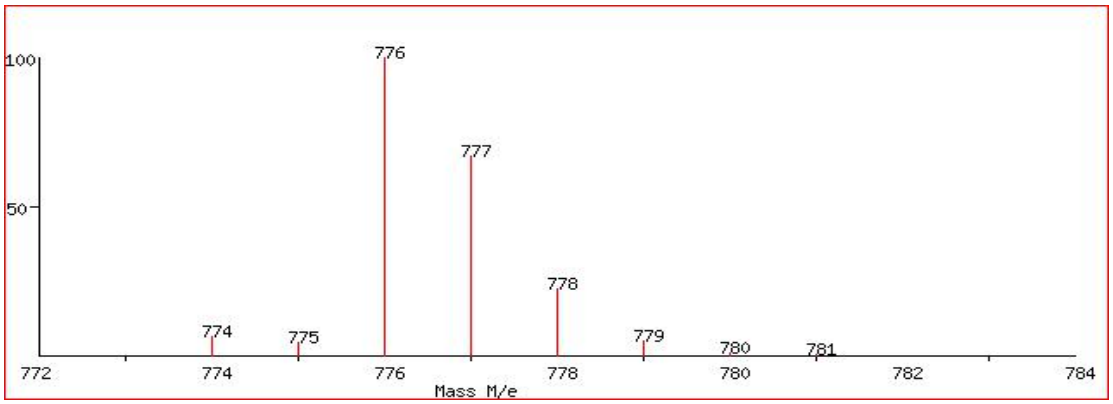
Figure. 18 The HPLC Chromatogram of Fe/Cu soot.



(a)



(b)



(c)

Figure.19 (a) The mass spectrum of the fraction that collected before 20 mins, measured at Oxford Chemistry Department, error(+/- 1). (b) The mass spectrum of the fraction came out the HPLC after 20 mins. The peak that indicated a molecular mass that is equal to that of Fe + C_{60} is highlighted by an arrow. (c) The predicted mass spectrum of Fe@C_{60}.

The difficulty of further characterization of this molecule was that the production of the raw soot was extremely slow. I found that the Fe oxide doped rods had a different texture compared to other rods. A resin might be used to make the rod, which impedes current conduction. It took about 5 hours to burn 1/10th of the rod. Hence it was very unlikely that we could produce enough materials for full characterization.

10.2 Functionalization of Endoherdal fullerenes

10.2.1 Introduction

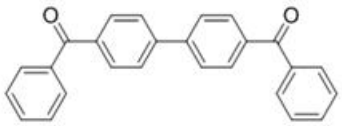
In order to realize QIP architectures, suitable and scalable technologies are needed to develop Qubits: the building blocks of a quantum computer.

One promising candidate system is spin-active endohedral fullerenes, such as N@C_{60}, or mono-metallofullerenes. These molecules allow the storage of information in electron spins and use electron-electron dipolar interactions to produce entanglement, a fundamental requirement for performing quantum operations. Coupling between spin-active molecules occur through electron-electron dipolar interactions [32], which are angle- and distance-dependent, therefore, in any array it is important to control both their spacing the relative orientation of molecules.[32]

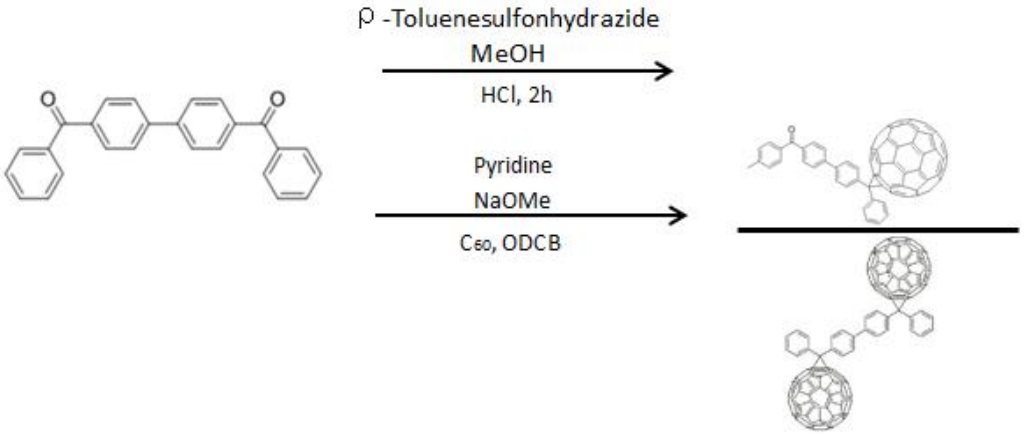
In this part of the work, efforts were made to address the first issue, i.e. maintain the space between the two molecules. A bridge molecule that was synthesized by Dr Xin Qian from our group was selected for this work as it provides a rigid structure to connect two fullerenes and main a fixed separation of them. In addition, the length of this chain can be engineered by adding/removing benzene rings which allows us close control of the distance between the two carbon cages.

10.2.2 EXPERIMENTAL SECTION

The bridge molecule selected to connect the two fullerene cages was custom made by Dr Xin Qian. The molecule is shown below and named M1.



50 mg of M1 and 25 mg ρ -Toluenesulfonhydrazide were dissolved into 5ml methanol, one drop of HCl was added and the resulting solution was then refluxed for 2 hours. The solvent was removed under vacuum. The resulting product was a white powder stuck on the walls of the flask. 10 ml of dry pyridine was added to the flask to dissolve the precipitate and 30 mg sodium methoxide was added quickly under nitrogen. The solution was stirred for 20 min. Meanwhile, 200 mg of C_{60} was dissolved into 15 ml dichlorobenzene(ODCB), which was then added to the stirred solution. The resulting purple solution was heated to 70-80 ^{o}C and stirred by a magnetic stirrer for 48 hours under nitrogen. Finally, the solution was refluxed for another 24 hours .



Scheme.2

10.2.3 RESULTS

The sample was purified by HPLC, The fraction that eluted between 5-6 min was collected and analysed by mass spectrometry (Figure 20). In the reaction C_{60} replaces one or two ketone groups to generate the monomer and dimer, respectively.

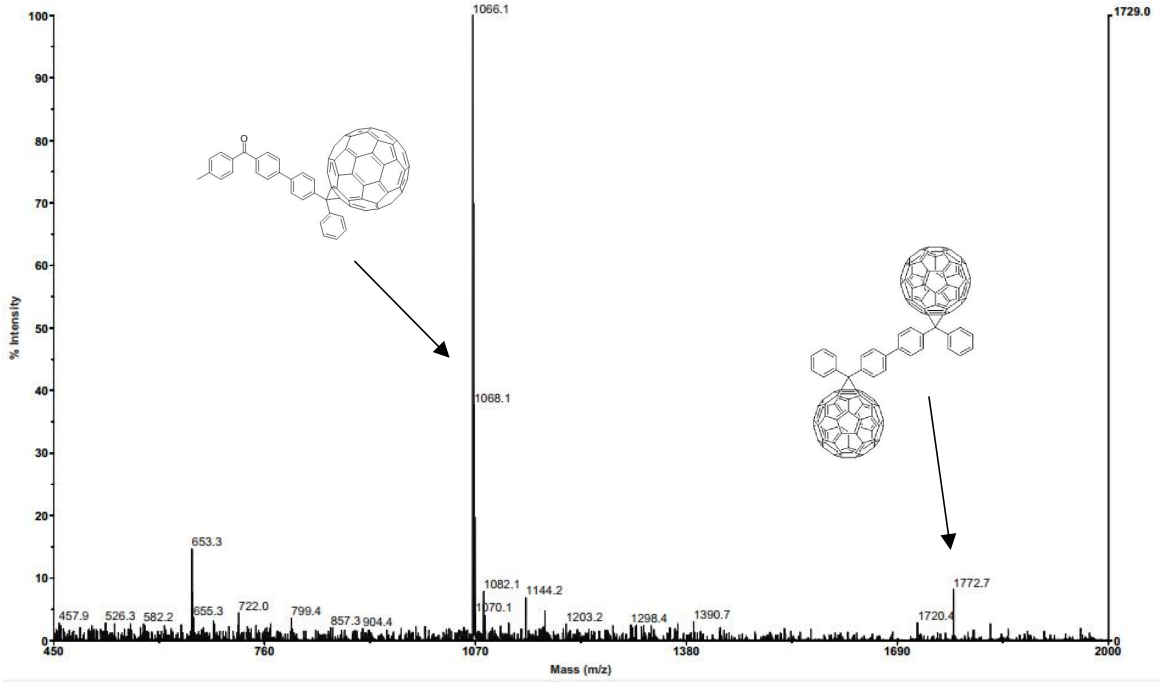


Figure. 20 The NMFS produced mass spectrum analysis of the functionalised sample.

10.2.4 DISCUSSION

Although the chemistry of C_{60} and $N@C_{60}$ is remarkably similar, this scheme cannot be transferred to $N@C_{60}$ as the long exposure of materials to elevated temperature can be detrimental of the spin signal of $N@C_{60}$. This is not a problem for $Y@C_{82}$. However, it was found that the $Y@C_{82}$ that was produced earlier degraded, and the Yttrium oxide doped rod in the lab had been used up, therefore it was impossible to produce more materials for this work. The transfer of this scheme to spin-active fullerenes may be performed in another project. In this trial, the molar ratio of M1, ρ-Toluenesulfonhydrazide and C_{60} was 1:1:2. The majority of functionalized produced was monomer, however, a small but noticeable amount of dimer had been produced as well. To increase the yield of dimer, higher proportion of C_{60} could be used.

10.2.5 CONCLUSIONS

A custom-made molecular bridge that allows us close control over the spacing between two fullerenes was selected to connect two C_{60} molecules together. Both monomer and dimer were produced successfully. However, Scheme. 1 was not further studied, as the functionalization of $Y@C_{82}$ was not possible within the timeframe of this project.

11. CONCLUSIONS AND FUTURE WORK

Endohedral fullerenes are remarkable molecules with unique electronic, magnetic and photovoltaic properties; they have found a number of application in various fields. Among all the potential applications, one particularly interesting application is to employ them as building blocks of quantum computer. The main factor that holds back scientific and commercial exploitation of these materials is their lack of availability in macroscopic amounts. This project was designed to address this issue, with specific attention paid to scaling up the production of $Y@C_{82}$ which is a spin active endohedral fullerene synthesized by the arc discharge method.

In Chapter 3, the typical EMF generation process with arc discharge was introduced and analyzed, the process was divided into 4 main steps and possible approaches to improve each step were discussed. A quantitative study of the Soxhlet extraction method was presented in Chapter 4. In this work, a much better understanding of Soxhlet extraction method had been obtained. A Soxhlet extraction scheme was developed in which the soot was pressed and packed as much as possible into the thimble. I found that replacing the solvent (DMF) every 20 hours was the most efficient way to extract the fullerenes. This extraction scheme allowed us to extract 95% of $Y@C_{82}$ from the soot within 60 hours, and a general pattern of this scheme had been revealed. This discovery has since been adopted in our lab to produce various endohedral fullerenes.

In terms of challenges, the biggest issue that I encountered in conducting this project was the occasional unreliability of the pilot arc discharge system which was the main facility of this project. As this is a pilot system, it was expected that some teething problems would be encountered. The failure of the rotating system, the melting of some valuable components, the occasional failure of pumps etc. caused some setbacks. Huge amount of time and energy were spent on restoring the arc discharge system and related facilities. However, my co-workers and I always got whole-heart support from the lab, our supervisor Dr Kyriakos Porfyrakis and the workshop in the department, which should be credited to the completion of this project.

Efforts were made to research the best conditions for generating $Y@C_{82}$ with the pilot arc discharge system. However, the first package of work was found to be flawed after a better understanding of Soxhlet extraction had been obtained. In the second work package, another set of data was generated and a 2^2 factorial design of experiments was employed to analyse the data. I discovered that both current and Helium pressure have positive effect to the yield of $Y@C_{82}$, while the combination of high values of current and He pressure has a negative effect to the production of $Y@C_{82}$. The relationship between

the yields and the parameters are more complicated than we imagined, however, I have shown that if a single parameter is to be analyzed, the yields of $Y@C_{82}$ can be increased by using high helium pressure.

Although fullerenes have been efficiently synthesized by evaporating carbon, the formation mechanism of these materials remains unclear. I discovered that classic formation scenarios like the "pentagon road" and "fullerene road" are inadequate to explain the synthesis of endohedral fullerenes in the arc discharge method. In chapter 6, I proposed that the production of fullerenes by arc discharge method adopts a "bottom up" scenario starting with the condensation of C_2, C_3 units. The precursors of empty cages and EMFs start to appear in the plasma at 32 carbon atoms and more than 44 carbon atoms in size, respectively. The branching of these clusters leads to a competition between the production of C_{60}/C_{70} and EMFs. Two main driving forces have been identified in the formation of fullerenes: closure of open structure to eliminate dangling bonds at earlier stage, and scaling up by incorporating C_2 units to release strain energy. I also provided further evidence to support that the formation of fullerenes adopts a so-called "closed network growth". My work provides a possible fullerene formation scenario in the arc discharge method, and a stepping stone to fully understand the formation of fullerenes. This work may also open new opportunities to tune the distribution of fullerene products in arc discharge method. The formation of fullerenes in the arc discharge follows a bottom-up scenario, and endohedral fullerenes (EMFs) are generated by scaling up smaller fullerenes without opening the cages.

The synthesis of fullerenes with the pilot arc discharge system allowed me to gain insights into the arc discharge synthesis and the pilot system itself. Attempts that were made to improve the efficiency and safety of the current system were introduced in Chapter 7. The realisation of the novel design of the arc discharge system or adopting selected concepts of the design may lead to more efficient production of fullerenes with arc discharge method.

In addition to the optimised Sohxlet scheme that was introduced in Chapter 4, further progress was made when a two-stage Sxohelt extraction/purification was independently discovered. This method employs two solvents (toluene and DMF) to extract fullerenes with different dipolar moment. This method was not only able to extract fullerenes effectively from the soot, but also to purify EMFs/TNT into high purity (97%) which significantly reduces the dependence on the tedious and laborious HPLC and speeds up the EMFs/TNTs generation process.

The Lewis acid separation method was reported to be an efficient approach to remove the empty cages from the EMFs[1], however, the efficiency and recovery rate of $Y@C_{82}$ were both lower than expected. I believe the main reason was because of the deposition of $TiCl_4$-EMF complex and the degradation of $Y@C_{82}$ cation as a result of exposing the $TiCl_4$ treated sample to air. This method is not suitable to be adopted into our fullerene generation process due to the lack of specific facilities in our lab. However,

the two-stage Sohxlet extraction/purification method had been proved to be able to reduce the dependence on the HPLC process.

In other chemistry work, I applied a functionalization scheme to C_{60} and a monomer and dimer were produced. This is encouraging as the scheme could be potentially transferred to $Y@C_{82}$. The successful transfer of this scheme to $Y@C_{82}$ will lead to a metallofullerene-based two-qubit system.

REFERENCES

1. Akiyama, K. *et al.* Non-HPLC Rapid Separation of Metallofullerenes and Empty Cages with $TiCl_4$ Lewis Acid. *J. Am. Chem. Soc.* **134,** 9762–9767 (2012).

2. Kroto, H. W. *et al*. C_{60}: Buckminsterfullerene. *Nature* **318,** 162–163 (1985).

3. Kroto, H. W., Tittel, F. K. & Smalley, R. E. Lanthanum Complexes of Spheroidal Carbon Shells. *J. Am. Chem. Soc.* 7779–7780 (1985).

4. Cioslowski, J., Fleischmann.E. D. Endohedral complexes: Atoms and ions inside the C 60 cage Not avaible for download. *J. Chem. Phys.* **94,** 3730 (1991).

5. Weiske, T., Böhme, D. K. ., Hrusak, J. ., Krätschmer, W. . & Schwarz.H. Endohedral Cluster Compounds: Inclusion of Helium within C_{60}: and C_{70}: through Collision Experiments. **30,** 884–886 (1991).

6. Chai, Y., Guo, T. & Jin, C. Fullerenes with metals inside. *Journal of Physical Chemistry.* **95,** 7564–7568 (1991).

7. Weiss, F. D., Brien, S. C. O., Smalley, R. E. & January, R. Photophysics of Metal Complexes of Spheroidal Carbon Shells. *J. Am. Chem. Soc.* **110,** 4464–4465 (1988).

8. Newell, C. Molecular Machinery with Fullerene Derivatives. (2013).

9. Brown, R. M. *et al.* Electron spin coherence in metallofullerenes: Y, Sc, and $La@C_{82}$. *Phys. Rev. B* **82,** 033410 (2010).

10. Iezzi, E. B. *et al.* A symmetric derivative of the trimetallic nitride endohedral metallofullerene, $Sc_3N@C_{80}$. *J. Am. Chem. Soc.* **124,** 524–5 (2002).

11. Lu, X., Feng, L., Akasaka, T. & Nagase, S. Current status and future developments of endohedral metallofullerenes. *Chem. Soc. Rev.* **41,** 7723–60 (2012).

12. Popov, A. a, Yang, S. & Dunsch, L. Endohedral Fullerenes. *Chem. Rev.* **113,** 5989–6113 (2013).

13. Godly, E.W, Taylor, R. Nomenclature and terminology of fullerenes : A preliminary survey. *Int. Union Pure Appl. Chem.* **69,** 1411–1434 (1997).

14. Averback, R. S.; Bernhoc, J.; Nelson, D. L., E. 1991; pp 627. Endohedral fullerenes. 2013 Review paper, reference 78. *Mater. Res. Soc. Pittsburgh* 627 (1991).

15. Letters, C. P. & After, I. A model for the C_{60} and C_{70} formation mechanism. *Chem. Phys. Lett.* **190,** 465–468 (1992).

16. Smalley, R. E. Self-Assembly of the Fullerenes. *Acc. Chem. Res.* 98–105 (1992).

17. Johnson, R. D.; Devries, M. S.; Salem, J.; Bethune, D. S. . & Yannoni, C. S. Electron paramagnetic resonance studies of lanthanum-containing C_{82}. *Nature* **355,** 239 (1992).

18. Kikuchi, K. *et al.* Isolation and characterization of the metallofullerene LaC82. *Chem. Phys. Lett.* **216,** 67–71 (1993).

19. Hayashi, N., Hashizume, T. & Sakurai, T. Direct STM Imaging of Spherical Endohedral $Sc_2@C_{84}$ Fullerenes. *J. Org. Chem.* **97,** 13438–13440 (1993).

20. Adachi, G.; Imanaka, N.; Fuzhong, Z. Handbook on the Physics and Chemistry of Rare Earths V. *Handb. Phys. Chem. Rare Earths* **22,** 61 (1991).

21. Lu, X., Akasaka, T. & Nagase, S. ChemComm Chemistry of endohedral metallofullerenes : the role of metals. *Chem. Commun.* **47,** 5942–5957 (2011).

22. Liu, F. *et al.* A series of inorganic solid nitrogen sources for the synthesis of metal nitride clusterfullerenes: the dependence of production yield on the oxidation state of nitrogen and counter ion. *Inorg. Chem.* **52,** 3814–22 (2013).

23. Stevenson, S. *et al.* Chemically adjusting plasma temperature, energy, and reactivity(e CAPTEAR) method using NOx and combustion for selective synthesis of $Sc_3N@C_{80}$ metallic nitride fullerenes. *J. Am. Chem. Soc.* **129,** 16257–62 (2007).

24. Tellgmann, R., Krawez, Z., Lin, S. ., Hertel, I. . & Campbell, E. E. . Endohedral Fullerene Production. *Nature* **382,** 407–408 (1996).

25. Aoyagi, S. *et al.* A layered ionic crystal of polar $Li@C_{(60)}$ superatoms. *Nat. Chem.* **2,** 678–83 (2010).

26. Murphy, T. A. *et al.* Observation of Atomlike Nitrogen in Nitrogen-Implanted Solid C_{60}. *Phys. Rev. Lett.* **77,** 1075–1078 (1996).

27. Morinaka, Y., Tanabe, F., Murata, M., Murata, Y. & Komatsu, K. Rational synthesis, enrichment, and (13)C NMR spectra of endohedral $C_{(60)}$ and $C_{(70)}$ encapsulating a helium atom. *Chem. Commun. (Camb).* **46,** 4532–4 (2010).

28. Murata, M., Maeda, S., Morinaka, Y., Murata, Y. & Komatsu, K. Synthesis and reaction of fullerene C_{70} encapsulating two molecules of H2. *J. Am. Chem. Soc.* **130,** 15800–1 (2008).

29. Kurotobi, K. & Murata, Y. A Single Molecule of Water Encapsulated in Fullerene C_{60}. *Science (80-.).* **333,** 613–616 (2011).

30. Gershenfeld, N. A. & Chuang, I. L. Bulk Spin-Resonance Quantum Computation. *Science (80-.).* **275,** 350–356 (1997).

31. Divincenzo, D. P. The Physical Implementation of Quantum Computation. *Fortschritte der Phys.* **48,** 771–783 (2000).

32. Harneit, W. Fullerene-based electron-spin quantum computer. *Phys. Rev. A* **65,** 032322 (2002).

33. Benjamin, S. C. *et al.* Towards a fullerene-based quantum computer. *J. Phys. Condens. Matter* **28,** S867–S883 (2006).

34. Morton, J. J. L. *et al.* Bang-bang control of fullerene qubits using ultra-fast phase gates. *Nat. Phys. 2* **1,** 40–43 (2006).

35. Porfyrakis，Kyriakos & Benjamin, S. C. in *Adv. Carbon Nanomater. Sci. Appl.* (ed. Tagmatarchis, N.) 2012 (Pan Stanford Publishing, 2012).

36. Krätschmer, W., Fostiropoulos, K. & Huffman, D. R. The infrared and ultraviolet absorption spectra of laboratory-produced carbon dust : evidence for the presence of the CbO molecule. *Chem. Phys. Lett.* **170,** 167–170 (1990).

37. Stevenson, S. *et al.* Small-bandgap endohedral metallofullerenes in high yield and purity. *Lett. to Nat.* **80,** 80–82 (1999).

38. Stevenson, S. *et al.* A distorted tetrahedral metal oxide cluster inside an icosahedral carbon cage. Synthesis, isolation, and structural characterization of Sc_4(mu3-O)$_2$@Ih-C_{80}. *J. Am. Chem. Soc.* **130,** 11844–5 (2008).

39. Stevenson, S. *et al.* Selective complexation and reactivity of metallic nitride and oxometallic fullerenes with Lewis acids and use as an effective purification method. *Inorg. Chem.* **48,** 11685–90 (2009).

40. Porfyrakis，Kyriakos & Plant, S. R. Patent EP2414284A2 - Methods and apparatus for the production of carbon containing materials. (2011).

41. Barrett, D. Synthesis and Functionalisation of Endohedral Metallofullerenes for Quantum Information Processing. (2013).

42. Krätschmer, W., Lamb, L. D., Fostiropoulos, K. & Huffman, D. R. Solid C_{60}: a new form of carbon. *Nature* **347,** 354–358 (1990).

43. Shinohara, H. Endohedral metallofullerenes. *Reports Prog. Phys.* **63,** 843–892 (2000).

44. S.Goroff, N. Mechanism of Fullerene Formation. *Acc. Chem. Res.* 77–83 (1996).

45. Ebbesen, T. W., Tabuchi, J. & Tanigaki, K. The mechanistics of fullerene formation. *Chem. Phys. Lett.* **191,** 336–338 (1992).

46. Khemani, K, K., Prato, M. & Wudl, F. A Simple Soxhlet Chromatographic Method for the Isolation of Pure C_{60} and C_{70}. *J. Org. Chem.* **57,** 3254–3256 (1992).

47. Bethune, D. S.; Johnson, R. D.; Salem, J. R.; de Vries, M. S. . Y. & S., C. Atoms in carbon cages- the structure and properties of endohedral fullerenes. *Nature* **366,** 123–128 (1993).

48. Diener, M. D., Smith, C. a. & Veirs, D. K. Anaerobic Preparation and Solvent-Free Separation of Uranium Endohedral Metallofullerenes. *Chem. Mater.* **9,** 1773–1777 (1997).

49. Nacalai USA. COSMOSIL Buckyprep-M. at <http://www.nacalaiusa.com/product.php?id=23>

50. Cumpson, P. & Sano, N. Stability of reference masses V: UV/ozone treatment of gold and platinum surfaces. *Metrologia* **50,** 27–36 (2013).

51. Borrill, H. Synthesis of N @ C $_{60}$ Derivatives for Quantum Information Processing. (2014).

52. Zhang, Q. L. *et al.* Reactivity of Large Carbon Clusters: Spheroidal Carbon Shells and Their Possible Relevance to the Formation and Morphology of Soot. *Phys. Chem. Lett.* **90,** 525–528 (1986).

53. Helden, G. Von, Gotts, N. G. & Bowers, M. T. Experimental evidence for the formation of fullerenes by collisional heating of carbon rings in the gas phase. *Lett. to natureNature* **363,** 60–63 (1993).

54. Irle, S. *et al.* From C_2 Molecules to Self-Assembled Fullerenes in Quantum Chemical Molecular Dynamics. *Nano Lett.* **3,** 1657–1664 (2003).

55. Chuvilin, A., Kaiser, U., Bichoutskaia, E., Besley, N. A. & Khlobystov, A. N. Direct transformation of graphene to fullerene. *Nat. Chem.* **2,** 1–4 (2010).

56. Zhang, J. *et al.* A missing link in the transformation from asymmetric to symmetric metallofullerene cages implies a top-down fullerene formation mechanism. *Nat. Chem.* **5,** 880–885 (2013).

57. Dunk, P. W. *et al.* Closed network growth of fullerenes. *Nat. Commun.* **3,** 855 (2012).

58. Johnson, R. D., Gerard, M., Salem, J. R. & Bethune, D. S. 2D Nuclear Magnetic Resonance Study of the Structure of the Fullerenes C_{70}. *J. Am. Chem. Soc.* **113,** 3619–3621 (1991).

59. Heath, J. R. Synthesis of C from Small Carbon Clusters A Model Based on Experiment and Theory. *ACS Symp. Ser. Am. Chem. Soc.* 1–23 (1992).

60. Feyereisen, M., Gutowski, M., Simons, J. & Almlöf, J. Relative stabilities of fullerene, cumulene, and polyacetylene structures for Cn : n=18–60. *J. Chem. Phys.* **96,** 2926 (1992).

61. Jing, X. & Chelikowsky, J. Nucleation of carbon clusters. *Phys. Rev. B. Condens. Matter* **46,** 15503–15508 (1992).

62. V.I.Kovalenko & A.R.Khamatgalimov. Electronic structure and stability of higher fullerenes. FULLERENES. *Nano Secur. through Sci. Ser. A Chem. Biol.* 437–441 (2007).

63. Lu, X., Li, H., Sun, B., Shi, Z. & Gu, Z. Selective reduction and extraction of $Gd@C_{82}$ and $Gd_2@C_{80}$ from soot and the chemical reaction of their anions. *Carbon N. Y.* **43,** 1546–1549 (2005).

64. Feng, L. *et al.* Structural characterization of $Y@C_{82}$. *Chem. Phys. Lett.* **405,** 274–277 (2005).

65. Khodorkovskii, M. A., Koltover, K. & Yagubskii, E. B. Novel proficient method for isolation of endometallofullerenes from fullerene-containing soots by two-step o-xylene– N , N - dimethylformamide extraction. *J. Mater. Chem.* **8,** 893–895 (1998).

66. Nagase, S., Kobayashi, K. & Akasaka, T. Endohedral Metallofullerenes_ New Spherical Cage Molecules with Interesting Properties, 1996.pdf. *Bull. Chem. Soc. Jpn.* **69,** 2131–2142 (1996).

67. Ruoff, R. S., Tse, D. S., Malhotra, R. & Lorents, D. C. Solubility of Ca in a Variety of Solvents. *J. Phys. Chem.* **97,** 3379–3383 (1993).

68. Saunders, M., Ha, J., Rj, C. & Rj, P. Stable compounds of helium and neon : He@C_{60} and Ne@C_{60}. *Science (80-.).* **259,** 1428–1430 (1993).

69. Saunders, M., Cross, R. J., Jimenez-Vazquez, H. a., Shimshi, R. & Khong, a. Noble Gas Atoms Inside Fullerenes. *Science (80-.).* **271,** 1693–1697 (1996).

70. Levitt, M. H. Spectroscopy of light-molecule endofullerenes Spectroscopy of light-molecule endofullerenes. *Philos. Trans. R. Soc.* **371,** (2013).

71. Morinaka, Y. *et al.* X-ray observation of a helium atom and placing a nitrogen atom inside He@C_{60} and He@C_{70}. *Nat. Commun.* **4,** 1554 (2013).

72. Wang, C. *et al.* . *Angew. Chem. Int. Ed. Engl.* **113,** 411–413 (2001).

73. Dunsch, L. *et al.* Metal sulfide in a C_{82} fullerene cage: a new form of endohedral clusterfullerenes. *J. Am. Chem. Soc.* **132,** 5413–21 (2010).

74. Stevenson, S. *et al.* Effect of copper metal on the yield of Sc_3N@C_{80} metallofullerenes. *Chem. Commun.* 4263 (2007).